CHARACTERIZATION OF DEVELOPING PORCINE CORTICAL BONE: APPLICATIONS OF MECHANICAL AND OPTICAL METHODS

BY

CORY LINDEMAN

THESIS

Submitted in partial fulfillment of the requirements
for the degree of Master of Science in Mechanical Engineering
in the Graduate College of the
University of Illinois at Urbana-Champaign, 2017

Urbana, Illinois

Adviser:

Professor Iwona Jasiuk

ABSTRACT

This thesis focuses on the characterization of developing pig bone under the effects of age-related changes and nutritional disease using several methods of characterization. The main characterization techniques are as follows: reference point indentation (RPI), compression testing, quantitative backscattered electron (QBSE) imaging, and nanoscale dynamic mechanical analysis (nanoDMA). The eventual goal of using this diverse set of characterization techniques is to understand and catalogue the changes that occur in bone due to biological factors. By understanding the various characteristics of bone, i.e. mineralization levels, property variations between quadrants, effects of disease, and microstructure variations, one can predict properties based on diagnostic knowledge.

The first study of this thesis is a partial review of the state of reference point indentation of bone. The origin of the device is explored, along with studies devoted to developing ideal operating conditions. Studies focusing on modeling RPI are also examined. Along with this literature review, an analysis of tip wear of the BioDent and Osteoprobe devices is presented.

The second study is a characterization of the mechanical effects on bone caused by induced colitis using three different measrement techniques. First, reference point indentation using the BioDent device was performed on femora and tibiae on both healthy and induced-colitis samples. Compression tests were completed on milled samples taken from cortical bones of left femora to determine modulus of elasticity and

ultimate compressive strength. Finally, bone samples were dried and ashed to determine porosity and bulk mineral volume.

The next study is a demonstration of the quantitative backscattered electron imaging technique (QBEI). This technique is applied to characterize the effect of age in developing bones on the hydroxyapatite mineralization percentage. The sample preparation technique and data analysis procedure are demonstrated for a general desired compound.

The final study of this thesis is an investigation using nanoindentation of the viscoelastic properties of the outer layer of bone, known as the periosteal bone, compared to the inner, or endosteal, tissue. NanoDMA was used to capture hardness, complex modulus, and tan-delta data at a distribution of frequencies from 10-200 Hz. Determining the difference in properties between periosteal and endosteal bone is crucial in understanding measurements taken by reference point indentation devices.

ACKNOWLEDGEMENTS

I wish to extend thanks to Professor Iwona Jasiuk for her assistance, guidance, and perseverance throughout my graduate career. Her time commitment towards my work and patience with me were monumental to my success. I would also like to thank Kathy Walsh of the Materials Research Lab and Scott Robinson of the Imaging Technology Group for their perseverance with equipment training and troubleshooting issues with me. Also, thank you to Peter Burks and the rest of the team at ActiveLife Scientific for providing the Osteoprobe and BioDent to be used by myself and the research group. Finally, thank you to my wife and family, whose support made this path possible.

TABLE OF CONTENTS

Chapter 1: General Introduction

Bone is a complex and hierarchical biological composite with many functions in the body. Due to its intricacies, many factors such as age, location, disease, and bone type can cause large variation in mechanical properties and composition. Thus, the main goal of this thesis is to catalogue these changes using a variety of methods. The results gained in the various works presented in this thesis also have application in the modeling of bone.

In this thesis, pig bones age zero to twenty weeks old are studied to determine the effect of age on properties. A second set of bones at three weeks old with both healthy and induced intestinal inflammation is studied to understand the effect of nutrient deficiency on bone.

Several methods are used to characterize the various properties of bone. Namely, a relatively new indentation method known as reference point indentation is used and examined. Reference point indentation (RPI) uses a two-part indentation tip that is set up to be useful in diagnostic situations. The details of the method will be discussed in the next chapter. A notable disadvantage of RPI is that it does not gather traditional mechanical properties, but specialized RPI parameters based on the indentation curve. To understand these RPI parameters, one must perform more traditional mechanical tests alongside RPI. For this purpose, compression and nanoindentation tests are performed as well. These tests are performed in an attempt to better understand what exactly RPI is measuring.

Alongside the mechanical tests, the technique of quantitative backscatter electron imaging (QBEI) is used to determine mineralization levels. This method is an electron microscopy technique that takes advantage of the interaction of the electron beam with surface atom nuclei. QBEI is able to accurately measure mineralization levels of bone at a very high resolution and allows for validation of the trends observed in mechanical tests.

The cataloging of property changes based on the presented factors allows us to more accurately predict clinical measures such as bone quality or fracture risk without direct measurement of the bone tissue.

Chapter 2: Review and Investigation of Reference Point Indentation

2.1 Introduction

In order to fully understand the reference point indentation method, a literature review and investigation of the relationship between test probe geometry and Osteoprobe measurement were performed. The literature review present in this chapter is part of a larger whole review of all facets of the technique. The review section presented here is focused on the initial development of the technique and further exploration of protocol for specific samples. The full review is an in-progress collaborative work between several research group members.

2.1.1 Introduction of RPI tools

The BioDent is an experimental tool created by Active Life Scientific meant for indenting both hard and soft tissues. The technique used by the equipment is called Reference Point Indentation (RPI). RPI differs from traditional indentation in that the indentation probe is composed of two independent probes. One probe, the reference probe, is first lowered into the sample to both provide a frame of reference for the second probe, and to keep the apparatus in a fixed position with respect to the sample. This leads to an advantage of RPI over traditional indentation techniques, as the sample is not necessarily required to be completely still – because all of the measurements are taken with respect to the reference probe, any motion of the test setup as a whole does not change the results, outside of noise effects. The second piece of the probe assembly is the second probe, called the test probe. This probe performs the major indentation on the sample.

There are currently three different configurations of probes available for use in the BioDent. Bone Probe 1 (BP1) is used for testing large bone samples with soft tissue present. This probe uses a sharp, beveled reference probe to anchor itself into the tissue. BP2, which is the most often used probe in the research community, uses a beveled reference probe similar to BP1, but with a flat end as to minimize damage to samples. BP3 features a reference probe that is completely flat in order to maximize contact area with the sample, which helps with stability during testing. This probe assembly type is used for very thin or fragile samples. All three probe assemblies utilize a conical test probe that ends in a spherical tip.

The motion of the probe assembly has several highly adjustable parameters to suit the need of an experiment. Controllable test parameters include number of indentation cycles, maximum indentation force, and frequency of indentations. These parameters can be controlled using the software provided with the BioDent Equipment to suit a variety of different experimental setups and sample types. Optimal values of the indentation parameters can possibly vary between sample types, which is an issue that will be discussed later.

To perform an indent using BioDent, the probe assembly is inserted into the sample to cause a reference load whose value is indicated by the software, depending on the indentation settings. Generally, the reference load is between half and one kilogram's worth of force. For consistencies sake, it is crucial that the sample is clamped or otherwise restrained so that there is no motion of the sample during the indentation cycles. Then, the user must dial in the correct touch-down distance (TDD) for the test probe. The TDD value is adjusted on the test head itself, and changes the initial distance of the test probe and sample surface. This setting ensures that there is sufficient travel distance for the test probe when performing indents. After this, the user can initiate the indentation cycles. As the BioDent performs its indents, it displays the force distance curve as the test is being performed. In general, most valid curves will look similar. Once the desired number of indentation cycles occurs, the BioDent software analyzes the force-displacement curves, and will instantly display up to five of the nine RPI parameters that were chosen by the user when setting up the test. Other curves such as time-displacement and time-force are available after the test, as well as any of the RPI parameters that were not selected to be displayed on the main results page. The user is then free to indent again on a new location or sample.

The nine parameters that the RPI technique produces are outlined in Table 2.1 below. However, some of the parameters are more interesting or offer more useful information about the sample. The parameters that most research is focused on currently are indentation distance increase (IDI), total indentation distance (TID), and creep indentation distance (CID).

Table 2.1: Definitions of Reference Point Indentation parameters

Parameter	Definition
CID1	Creep indentation distance of the first cycle
ID1	Indentation depth of the first cycle
US1	Unloading slope of the first cycle
IDI	Indentation distance increase, difference between first and last indentations
TID	Total indentation depth
AvCID	Average creep indentation distance over every indentation cycle
AvED	Average energy dissipation, starting from third indentation cycle
AvLS	Average loading slope of all indentation cycles
AvUS	Average unloading slope of all indentation cycles
BMSi	Bone Material Strength. Ratio of indentation distance in sample to indentation distance in PMMA standard. Only parameter given by Osteoprobe

Something to note is that these parameters are unique to the RPI technique and do not include traditional mechanical values such as modulus, hardness, or fracture toughness. One of the major research focuses on the RPI technique has been correlating the RPI parameters with traditional mechanical parameters, or understanding what exactly these RPI parameters are measuring about the sample's mechanical properties. As of this publication, there are many conflicting opinions on whether or not the RPI parameters have any mechanical significance at all, but there is notable evidence that TID, IDI, and CID are the three most important parameters that can be related to traditional mechanical parameters.

The Osteoprobe is a handheld microindenter device that is also developed by Active Life Scientific. Active Life Scientific boasts that the Osteoprobe is the first and only easy-to-use device that directly measures in-vivo properties of bone directly This device works on the same principle as the BioDent, that is, it uses reference point indentation. This comes with both the benefits and the downsides to the RPI technique - the areas that can be tested are quite robust due to the two-probe setup, but it is unknown what exactly is being measured by the device. This device is meant mostly for clinical use, so its operation is greatly simplified when compared to the BioDent. Thus, the indentation procedure is not as customizable as BioDent. One significant difference between the two devices is that the Osteoprobe performs RPI without the use of a reference probe. In lieu of the reference probe, the reference point is taken as right before the device actuates the indentation.

The Osteoprobe performs only one indent at a time, at a set force of 40 N. Otherwise, operation of the Osteoprobe is very similar to the BioDent. First, a reference load of 10 N must be applied to push the test probe through any soft tissues that are on top of the bone. This serves as any preconditioning of the sample that could be needed. It is important for the operator to keep the Osteoprobe at a +/- 10-degree angle from perpendicular from the testing area in order to perform a good measurement. However, Active Life Scientific states that an individual with no prior experience with using the Osteoprobe can be trained to perform good measurements in about an hour.

As opposed to the BioDent, the device performs only a single indent. As with the applied force, this value is not able to be changed. Once the indent has been performed, the Osteoprobe gives one parameter – the Bone Material Strength Index (BMSi). The BMSi is a ratio of the sample indentation distance to the indentation of a standard PMMA sample. Against a standard PMMA sample, the Osteoprobe is assumed to indent a distance of 150 microns. This distance is used to normalize whatever distance is indented in the desired material to calculate the BMSi of the sample. Active Life Scientific recommends at least 5 indentations per sample due to statistical and consistency reasons.

Because the Osteoprobe only performs a single indent, there is some information such as dynamic properties of the sample that is lost when comparing to a BioDent test. Because this information is being lost, there is very little relationship between results from the two tools. Current research using the Osteoprobe is focused on documenting the changes that the BMSi of bone has under various physiological differences such as age, disease, and activity level. Due to its ease of use and smaller form factor, the Osteoprobe is often chosen over the BioDent for live-subject studies.

It should be noted that the two tools presented are quite different in their intended application and information output. However, some recent publications have been fairly loose in their assumptions between the two devices. Thus, the purpose of this review - to clarify differences between applications of each device, and demonstrate to the best of our knowledge the current state of affairs when it comes to the RPI technique.

2.2 Literature Review

2.2.1 Publication History

In the past few years, the study of RPI has become more popular due to the first clinical applications of RPI. The ability to directly measure mechanical properties in-vivo without any lasting side effects is convenient and effective. The introduction of the technique (Osteo-probe), written by Hansma, appeared in 2006 [1]. The first human clinical experiments were done by Diez-Perez in 2010 [2]. He studied the bone mechanical properties of human in vivo. Later on, the first RPI paper (BioDent) that used animal as well as human in vitro samples was published in 2012, which used RPI to determine the effect of freezing on bone mechanical properties [3]. Papers that used or studied RPI have emerged quickly since 2013. The studies of bones using the RPI technique are still increasing. As of July 2017, 73 papers have been published using reference point indentation in some form. Among all the papers that utilize the RPI technique, researchers most often choose to use animal samples due to ease of acquisition and ability to control variation in bone quality.

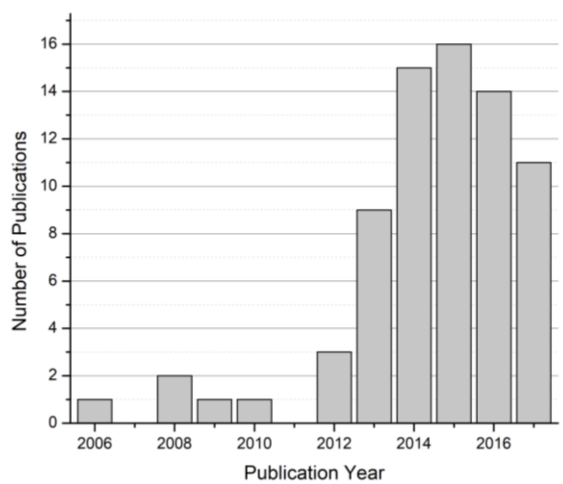

Figure 2.1: Number of Publications per year involving reference point indentation

2.2.2 Development of Reference Point Indentation Technology

The first publication involving the RPI technique was published in 2006 by the inventor Paul Hansma and his research group [1]. This first paper presents what was known as the "Bone Diagnostic Instrument" at the time. This early prototype resembles the Osteoprobe much more than the BioDent, as it was presented as a handheld device rather than the mounted version of the device. This publication presented the proof of concept of the RPI technique. Hansma and his group showed that data taken from the BDI showed significant differences between baked and control bovine bones. Baking was used to deteriorate the organic phase of the material to significantly change its mechanical properties. The indentation increase (IDI, but not named in this publication) of the baked bovine bone is significantly higher than of the control bone. Additionally, the IDI of bone from older donors (59 y.o.) was higher than younger donor bone (19 y.o.). They also demonstrated that the effect of testing is only present during the first several indentation cycles. This proves that in-vivo and live-subject tests are possible without corrections to account for soft tissue, so long as a sufficient number of indentation cycles are done.

The second paper in the series presents the second version of the bone diagnostic instrument [4]. The new version starts to resemble the BioDent product we know today, with the option to mount the test head onto the indentation bed. This paper presents more proof of concept experiments that show the capabilities of the bone diagnostic instrument. IDI of irradiated bone (meant to weaken fracture toughness) was significantly higher than that of control samples. Another age study was done to compare mature bone (17 y.o.) to elderly bone (79 y.o.). Once again, the IDI of the elderly bone was shown to be higher, showing again that the IDI can correlate to fracture toughness of bone. 4-point bending tests were also done on these samples, but no correlation was found between any of the traditional mechanical parameters and IDI in this experiment. This paper also introduced and tested a new parameter called the Repetitive Indentation Resistance (RIR), defined to be the inverse of IDI. This parameter was introduced to have a parameter that was positively correlated with bone toughness as opposed to negatively correlated, like IDI. After statistical testing, IDI correlated more closely with the toughness value of the tested samples, so the concept of the RIR never made it past this publication.

A third paper was published by Randall of the Paul Hansma research group in the series of introductory papers of the RPI method and the Bone Diagnostic Instrument [5]. This study focused on demonstrating the effectiveness of the BDI on mouse bones, rather than the larger bones the previous studies focused on. The effect of age of rats (19-week vs 19 month) and exercise level of each age group was studied, mostly focusing on changes of IDI.

Comparing the age groups, the IDI of young bones was significantly ($p < 0.0003$) lower than of old bones, which is to be expected from previous studies. For the young group, rats who were exercised regularly also had a significantly lower ($p<0.0004$) IDI than the control group. However, for the old group, the difference between control and exercised rats was noticeable, but not statistically significant. What is interesting about these results is that modulus or hardness did not change between any of the test groups. While differences in fracture toughness would be possible to measure using traditional fracture toughness tests, only the BioDent and Osteoprobe have the capability to detect these fracture properties in-vivo.

In summary, the first publications by the Hansma group show the initial promise of the RPI technique. The ability to differentiate between different affected tissue samples and the ability to sense changes through tissue with little change in the statistics of the data show great promise in the area of clinical testing. By compiling a catalogue of results from different bone types (age, disease, etc.), BioDent and Osteoprobe could be used as a diagnostic tool rather than just a direct measure of bone properties.

2.2.3 Development of Reference Point Indentation Protocol

Due to the large number of customizable parameters in the RPI method, large variation of measurement techniques between studies is inevitable. In order to normalize results between research groups, a set of standard settings for specific samples is necessary. This development of standard settings is a focus in large amount of studies done.

Setters performed a variety of measurements aimed to determine the effect of sample preparation on the nine RPI output parameters [6]. Statistical analysis was performed to determine the best ways to reduce deviation of RPI parameters by preparing and testing the sample in certain ways. The following variations were tested for using Tukey tests and ANOVA: indentation force, number of indent cycles, longitudinal or transverse sample surfaces, effect of polishing, irradiated samples, and comparing two samples cut from two genetically similar animals.

For force variation, all parameters linearly increased with force except for IDI, which exhibited a cubic increase. Setters proposed that the linear behavior is caused by increased loading rate, as loading time was held constant. Number of cycle variation showed AvED and AvCID having downward asymptotic trend, IDI and AvLS upward asymptotic behavior, while all other parameters remained relatively constant.

Preconditioning has little effect on parameters, only on those that are measures of first indents – which is to be expected. The benefit of multiple indent shows in this test. The fact that preconditioning is not needed when larger indentation numbers is performed is one of the positives of using RPI over traditional indentation techniques.

Polishing of samples was shown to greatly decrease variation of parameters. All parameters were significantly different between polished and unpolished longitudinal samples. Polished samples between transverse and longitudinal direction have minor differences for all parameters except IDI and AvED. Micro-CT radiation, often used as imaging for numerical simulations of bone samples, only showed variance on US1, AvUS, and AvLS on transverse samples. Differences between samples were not statistically significant.

Jenkins published a protocol study similar to the Setters paper studying the variability of RPI parameters caused by sample preparation and experimental setup [7]. The following variables of sample preparation were studied: sample orientation, surface preparation, presence of soft tissue, and sample thickness. In particular, this publication focused on novel studies on experimental variables that had not been studied in the past. Experimental variations in maximum load, measurement spacing, and mode use were studied as well. The RPI parameters of interest in this study were IDI, CID, and TID.

As a result of the study, the authors were able to build a set of recommendations to reduce error in RPI measurements. A minimum of 8-15 measurements per sample should be made to keep error below the 5-10% range. Sample thickness should be at least 10 times the indentation distance, which is a standard rule in most indentation applications. Periosteum and the immediate surface of the bone should be machined away in order to probe the osteonal tissue properties. Indents should be performed with a minimum spacing of 0.5 mm. This distance is limited by the size of reference probe. Jenkins recommends focusing on IDI and CID as the main RPI parameters, but also TID if the touchdown point is clear on the data.

The first publication showing applications of the Osteoprobe was released in 2013 by Randall of the Hansma Research group [8]. The purpose of this study was to demonstrate the capabilities of the new handheld RPI device in clinical settings. Calibration tests were performed on bare bone, tissue covered bone, and PMMA. In-vivo tests were also performed on horse and human patients. Results showed that BMS was largely unaffected by the presence of tissue on the testing area, which speaks well of the Osteoprobe's main purpose – an easy to use device meant for clinical settings.

A second paper showcasing the Osteoprobe's method was published by Lescun of the Hansma research group in 2015 [9]. This work, focusing on varying indentation conditions on samples from horses' third metacarpal (lower leg bone), explores the effect on the BMSi measurement from a multitude of different variables. Means of each sample group's BMSi were compared using mixed-mode ANOVA tests to test if varying each condition had a significant effect on the measurement. The following variables were tested: age, sex, limb, bone region, and surface condition of bone. Bone region was varied between the proximal, diaphysis, and distal regions of bone, as well as medial and lateral quadrants. The test surface was varied between testing live subjects, recently euthanized subjects, testing through skin, and indenting on bare bone. Tests from the varying surface conditions were only compared using equivalent location on the bone.

Of the studied parameters, sample sex, limb variation, and quadrant variation had no significant effects on BMSi measurements. Body weight was shown to have a linear relationship with BMSi. Based on the knowledge of bone remodeling due to varying loads, this observation seems logical. When comparing measurements on live subjects to measurements performed on recently deceased animals, means were slightly different, but not statistically likely to be. This is a significant result for the Osteoprobe in terms of veterinary diagnostic applications, as BMSi can be used as an emergency diagnostic tool in cases when a fracture must be investigated. BMSi was also measured to be larger in adult samples compared to foal samples. This reflects results obtained and discussed later in this chapter on porcine samples. The other two indentation conditions, through skin and on exposed bone, have a minor but significant difference in adult samples. However, this is easily accounted for if necessary. A similar effect occurs in adult samples when comparing distal versus the diaphysis of bones. Distal indentations, compared to indentations on the diaphysis and proximal, have lower BMSi, but are not statistically significant.

Krege published a study in an attempt to understand variation of RPI parameters under changes of mechanical properties due to chemical treatments in 2016 [10]. The treatments are as follows: dried to remove fluid, dried and ashed to remove any soft tissue, demineralized, and soaked in raloxifene to improve toughness and hydration. Overall, this study shows some inconsistencies in the reference point indentation parameters with regards to changes in mechanical properties. For example, the IDI and TID of ashed bones were shown to be lower than of pre-treatment bones. Ashing has been shown to be a simple way to decrease bone toughness, which was verified by 4-point bending tests here. This also differs from results from a previous Hansma paper [1].

In demineralized bones, it was shown that the surface of the sample was disproportionally affected compared to the bulk material. RPI properties were increased at a larger degree compared to bending measurements due demineralization being a surface-oriented treatment. This has no direct physiological relevance, but this effect should be taken into consideration when studying any physiology that is present in bones' outer surface, such as remodeling. Previous studies have shown that lower bone toughness is correlated with increasing IDI, while this study shows that this is not always the case. Further study is necessary to understand the complexities of the relationship between mechanical properties and RPI parameters.

The protocol papers discussed present an interesting challenge in using the BioDent and Osteoprobe - the amount of customization available for a test is quite extensive. This makes studies done by different research groups difficult to compare if different settings were used. Protocol papers help to determine the most optimal settings to decrease the variability in the data. The need for a set of standard settings for different types of samples is quite clear.

A powerful method to assess the effect of mechanical properties on reference point indentation parameters is finite element analysis (FEA). The ability to directly assign material properties with controlled geometry helps to alleviate the issue of significant variability in biological materials. However, FEA of reference point indentation is an underexplored area of study, with only two studies published as of July 2017.

Hoffseth of the Hansma group published the first study of finite element analysis of RPI in 2014 [11]. The indentation profile of experimental indentations measured by atomic force microscopy is compared to simulated indentation profile in an effort to validate predictions on the effect of tip sharpness. The two tip radii measured are classified as sharp (< 15 microns) and blunt (~ 35 microns). FEA results were comparable with AFM measurements only after introducing a reduction of modulus along the loading of tissue to simulate tissue degradation.

The second publication concerning FEA of RPI was published by Idkaidek in 2016 [12]. This study created an FEA model of the BioDent in an effort to predict RPI parameters based on changes of four mechanical properties and three indentation properties available to change in the BioDent software. Table 2.2 outlines the varied parameters and the determined correlations with each RPI parameter. All relations presented in this study are determined to be linear.

Table 2.2: Summary of Correlations of RPI Parameters from Idkaidek (2017)

	ID 1st	US 1st	LS 1st	CID 1st	TID	IDI	AvCID	AvUS	AvLS	AvED
Young's Modulus	↓	↑	↑	-	↓	-	-	↑	↑	-
Compressive Yield Stress	↓	-	↑	↓	↓	↓	↓	↓	-	↓
Damage Constant	↑	↓	↓	↑	↑	-	-	↓	↓	↓
Viscosity Constant	↓	↑	-	↑	↓	↑	↑	-	-	↑
Indentation Force	↑	↑	↑	↑	↑	↑	↑	↑	↑	↑
Indentation Probe Radius	↓	↑	↓	↑	↓	↑	↑	-	-	↓
# of Indentation Cycles	-	-	-	-	↑	-*	↓	↓	↑	↓

An increase of elastic modulus, as expected, leads to an increase of the loading and unloading slope parameters (US 1st, LS 1st, AvUS, AvLS). The unloading slope parameters are very strongly correlated to elastic modulus, which is useful in predicting changes in stiffness by measuring US 1st and AvUS. Interestingly, the first cycle indentation distance is decreased. This is likely to be explained by increased stiffness limiting plastic deformation of the first indentation cycle, which has a large amount of plastic deformation and damage. Increasing the compressive yield stress decreases the distance parameters (ID 1st, TID, and IDI), the creep parameters (CID 1st and AvCID), average unloading slope and energy dispersion, as well as increasing the first loading slope. Lowering the compressive yield stress leads to a decrease in material compliance, which fits these observations of parameter correlations. The correlations with the damage constant imply that the majority of damage that occurs in reference point indentation happens in the first indentation cycles. An increase of the viscosity constant increases the time-dependent parameters (CID 1st, AvCID, and AvED), as well as US 1st, and IDI. Indentation force increases all parameters due to increased damage and indentation depths. Variation of probe radius is a key factor to track due to blunting of the tip through indentation. Increasing the number of indentation cycles had loosely correlated effects on the shown parameters.

This extensive compilation of correlations is a crucial step in understanding the connection between traditional mechanical measurements and parameters measured by reference point indentation.

2.3 Investigation of Osteoprobe Tips & Measurements

In an effort to understand both the use of the Osteoprobe and the mechanical changes present in young porcine bones, a series of indentations was performed on six age groups of bones from 0 weeks old to 20 weeks old. The indentation radius was also measured before and after indentation in order to track deformation of the tip. Understanding the deformation of the tip is an important part of modeling reference point indentation, as shown in the Idkaidek publication discussed above. Tip radius has been shown to affect BioDent parameters, so it can be assumed that BMSi measurements performed using the Osteoprobe are affected as well. This work also serves as a basis of comparison for the multiple tests performed on the same sample group discussed in further chapters of this thesis.

2.3.1 Age-Effect Study of BMSi Measurements

To indent on bone, samples were cut from mid diaphysis of tibiae using a band saw. The size varied per age group such that a ratio of sample size to total bone length was kept relatively constant. Samples were previously stored at -20 °F wrapped in PBS-soaked gauze. Prior to indentation, samples were defrosted at 34 °F for at least 24 hours. During indentation, the samples were clamped to avoid movement caused by indentation forces. As directed by ActiveLife Scientific, indentation protocol was 10 indents on the sample, followed by 10 indents on the PMMA control sample. The time per indentation to compress the Osteoprobe casing was at least one second per indent, while holding the device within +/- 10° perpendicular to the sample. Bone samples were also kept hydrated using PBS until indentation occurred. For consistency, the anterior quadrant was indented for each sample.

Figure 2.2 shows the result of three runs of 10 indentations each on the six age groups. Using a one-way ANOVA test performed on OriginPro 8.5, the mean of each run was compared for each age group. The 8, 12, 16, and 20-week-old age groups were all predicted to have equal means across all three runs. The 0 and 4-week-old sample groups had one run with significantly different mean BMSi than the other two runs. The 12-week sample group has only two runs of data due to measurements marked unacceptable by the Osteoprobe software.

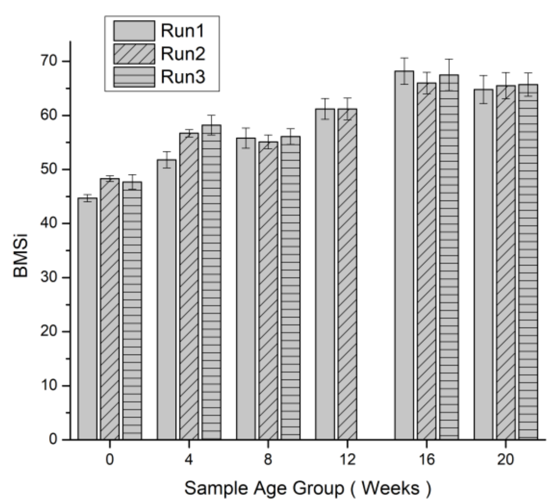

Figure 2.2: BMSi measurements across six age groups

Overall, the data shows that the variability of measurements is low outside of young bone, provided the measurement technique is consistent with the suggested usage. To more effectively compare average values, the runs with statistically equal means were combined for each age. Figure 2.3 shows these new values.

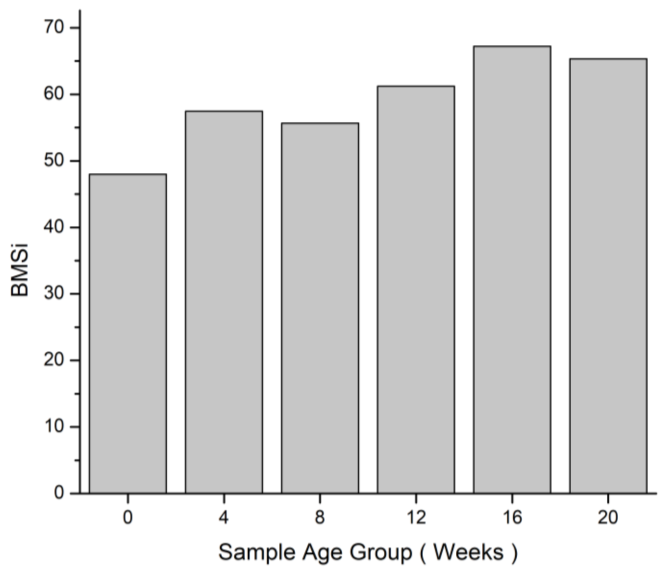

Figure 2.3: Average of equal-mean runs of BMSi measurements

With regards to age, the pattern presented is linear as expected. The means of the 16 and 20-week-old sample groups are statistically similar, which may suggest that there is a leveling-off of BMSi at the later ages of the study. It would be wise to investigate further to see of the pattern is continually linear or it does in fact level off.

2.3.2 Imaging of Osteoprobe

The Osteoprobe tips used in the above age-effect study were imaged in an electron microscope before and after indentation. For imaging, a FEI Quanta FEG 450 SEM was used, courtesy of the Imaging Technology Group at the Beckman Institute. An accelerating voltage of 20 kV and spot size of 4 microns was used to image the tips. After imaging, the indentation tips' radius of curvature was measured using a custom MATLAB program.

Nine tips that were used in the above age study were imaged before and after indenting samples. The average tip radius before indenting was measured to be 2.31 +/- 0.75 microns, with a median value of 1.54 microns. After indenting, the mean value was measured to be 5.17 +/- 1.09 microns, with median value of 5.16 microns. Table 2.3 displays some extra statistics of the measured radii.

Table 2.3: Summary of Osteoprobe indentation tip radii (all values in microns)

	Mean	Standard Error	Median	Minimum	Maximum
Before Indentation	2.312	0.749	1.540	1.005	5.421
After Indentation	5.173	1.086	5.159	2.748	9.172

Tip radius increase was plotted against the average BMSi measurement that the tip performed to check for trends. To normalize, percentage increase from initial radius was also calculated and plotted against BMSi measurement. These plots are shown in Figure 2.4.

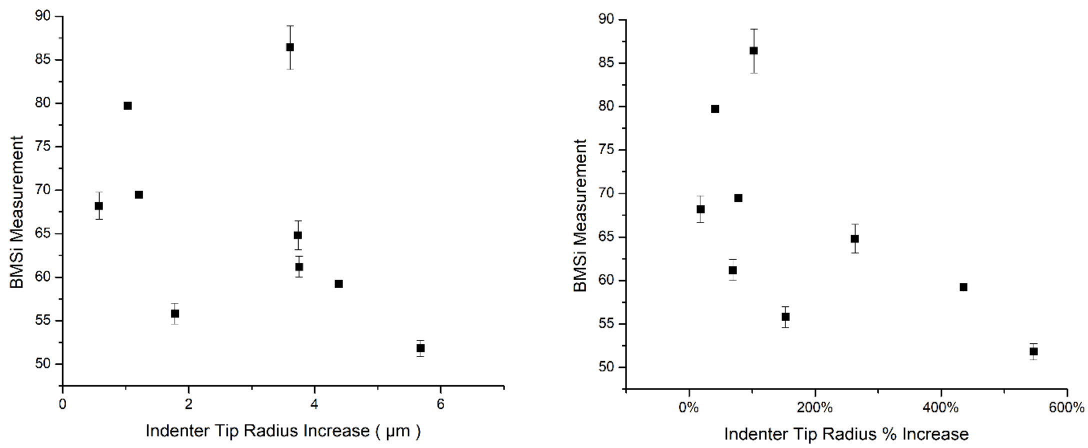

Figure 2.4: Plots of indenter tip radius increase plotted against measured BMSi

Overall, the trend for both the radius increase and normalized percentage increase are roughly inversely related to the measured BMSi. However, the linear correlation for both plots is very low, with r^2 values of 0.1714 and 0.3904 respectively. It would be worthwhile to explore other materials with BMSi with values higher than the samples studied in this work to see if the trend continues.

2.4 Conclusions

In conclusion, reference point indentation is a promising technique with an ever-growing number of studies dedicated to understanding its significance. Most studies show positive results for relationships between traditional mechanical properties and RPI parameters. However, some studies demonstrate that this relationship is not as simple as assumed by some works, with previously assumed patterns not occurring in all cases. Finite element analysis has proven to be an effective method alongside experimental correlation to predict trends of RPI parameters. Overall, RPI has shown to be very effective in potential diagnostic situations, but can be explored further.

A small study of the age-effect in developing porcine bones was also performed. The Osteoprobe proved effective in identifying the increase of mechanical quality of bone via increasing BMSi. The indentation radius was also tracked before and after indentation on bone. The increase in tip radius tended to decrease for indentations performed on bone with higher measured BMSi, but the correlation was relatively low and has room for further exploration.

Chapter 3: Reference Point Indentation and Mechanical Testing of Induced-Colitis Bone

3.1 Introduction

3.1.1 Introduction to Colitis

Bone properties such as stiffness and strength are partly determined by the degree of mineralization of the bone. In order for a bone to form properly throughout development and aging, the appropriate amount of minerals must be transferred from food intake. Without proper mineral intake and absorption, reduced bone mineralization content leads to reduced bone growth and mass [13]. There are many causes of impaired bone mineralization, including inflammatory bowel diseases (IBD) [14].

One example of an IBD that affects bone growth is colitis. Colitis is a form of digestive disease characterized by an inflammation of the colon. It affects bone growth by limiting bone mineralization. Colitis prevents the normal absorption of nutrients, including the minerals needed for bone growth [15]. The loss of mineralization caused by colitis increases the risk of bone growth retardation as well as metabolic bone disease (MBD), which is characterized by an increase in bone fragility and bone demineralization [13, 16].

Currently, the long-term effects and consequences of MBD are unknown. Lower bone mineral content (BMC) and bone mineral density (BMD) prevent bones from reaching their peak bone mass, and also increase the possibility of the development of premature osteoporosis [17, 18]. Several studies have been done on the mechanisms of induced colitis in mice, but in swine or human the disease is relatively uninvestigated, as well as secondary effects of the induced colitis [18]. This study demonstrates that there is a similar mechanism of induced colitis from dextran sodium sulfate in swine. An investigation into mineral structure and physical integrity of piglet long bones has been performed by another group [19], with similar goals to this study, although with different measured properties.

3.1.2 Overview of RPI

One unique approach of this study is the use of a special indentation technique known as reference point indentation. Developed by ActiveLife Scientific, the BioDent and Osteoprobe devices use reference point indentation (RPI) as a means to test physical properties of biological material. This work is focused on using the BioDent device to test the colitis-induced samples, which has been demonstrated to be able to differentiate healthy and diseased bones in several cases [1, 4, 5]. The BioDent uses a cyclic indentation pattern and special software to determine nine RPI parameters to characterize the material. These nine parameters are unique to the RPI method. The most significant for this work are the indentation distance increase (IDI), total indentation distance (TID), and creep indentation distance (CID), but all parameters will be presented. Definitions of the RPI parameters are presented in the references above. Another device manufactured by ActiveLife Scientific, the Osteoprobe, was also used to test the bones [8]. However, both the control and DSS-treated samples were too soft to trigger the measurement threshold of the Osteoprobe.

3.2 Methods

3.2.1 Animal study

All animal care and experimental procedures were in accordance with the NRC Guide for the Care and Use of Laboratory Animals and were approved by the University of Illinois Institutional Animal Care and Use Committee. Thirteen two-day old piglets (postnatal day – PND2) were brought to the animal rearing facility and were acclimated for 12 days. Piglets were fed commercial non-medicated sow-milk replacer formula (Advance Liqui-Wean, Milk Specialties Co., Dundee, IL, USA) which was formulated to meet or exceed 2012 National Research Council requirements for 3-5 kg piglets. Piglet body weight (BW) was recorded to determine milk volume to be dispensed to individual animals. Diets were prepared daily and piglets were fed at the rate of 295, 310 and 325 mL/kg BW starting on PND 2, 5 and 8 respectively. Formula was delivered to piglets 12 times/day via a peristaltic pump.

3.2.2 DSS-induced Colitis

Colitis was induced with the use of dextran sodium sulfate (DSS; MW: 40,000-50,000; Affimetrix, Inc, Santa Clara, CA) with a modified protocol described by Young et al. [20]. Briefly, on PND14 through PND18 (or day 12-16 of study), eight animals were dosed with, 1.25 g DSS/kg body weight. DSS was prepared as 20% solution in phosphate buffer saline (PBS) prior to gavage and poured into individual piglet feeding bowl. The remaining 5 animals received similar volumes of PBS alone and served as controls. Rectal temperature and stool consistency were assessed daily after DSS dosage. Evidence of colitis was detected by the presence of bloody stool or diarrhea.

3.2.3 Sample collection

Tissue collection took place at two points: on PND19 or 1 day after the end of DSS treatment, three colitis animals were euthanized to assess early impact of colitis on bone structure; the remaining animals from both control and colitis groups were euthanized on PND23. Large intestine samples were collected and were either snap-frozen in liquid nitrogen or fixed in formalin to confirm intestinal inflammation. Bone samples dissected from the body and scraped from any tissue. They were then wrapped in gauze soaked in PBS for preservation and frozen at approximately -20 °F.

3.2.4 RPI Samples

For RPI testing, each of the twelve sets of bones were indented five times per sample with BP2 reference probes, totaling 40 indentations for colitis bones and 20 indentations for control samples. Indentation protocol was as follows: 6 N indentation force, 2N preload, 10 indentations per cycle, and 2 Hz indentation frequency**.** To prepare the samples for indentation, soft tissue was scraped away from the bone ensuring not to damage the surface. Whole bone samples were indented on the posterior side near the diaphysis to test a representative region of each bone.

3.2.5 Compression Samples

Compression samples were cut using a diamond saw from concentric bone samples from left femora. Sample cross sections were square with height to side length aspect ratio 3:2. Nineteen samples were cut from control bones and 13 were cut from treated bones. Compression was performed on an MTS Insight equipped with a 2000N load cell, and running TestWorks4 EM V4.11B. Samples were loaded at 1 mm/min until significant plastic deformation such that ultimate stress was reached, or fracture occurred.

3.3 Results

3.3.1 DSS-induced colitis

DSS treatment did not affect formula intake, weight gain or rectal temperature. Diarrhea (stool consistency ≥3 out of 4) was observed in >80% of piglets within 2 days of DSS treatment, but then decreased as the study progressed. Blood was observed in the stool of 1/3 of DSS-treated piglets on PND19 which progressively increased to 100% by the end of the study (PND23). Localized colonic inflammation and morphological changes in DSS-treated piglets compared to control (data not shown) confirmed the development of colitis in DSS-treated animals.

3.3.2 Reference Point Indentation Results

RPI was performed on right tibiae and femora to determine differences of indentation parameters between the treated and control groups. Tibiae and femora were used to test if difference between test groups were consistent throughout the skeleton. Results of the nine RPI outputs are grouped into four categories based on units. (Figures 3.1-3.8). An unpaired t-test assuming unequal means was performed on the results using OriginPro 8.5. For each RPI parameter, difference between mean values of treated and control bones were found to be statistically significant.

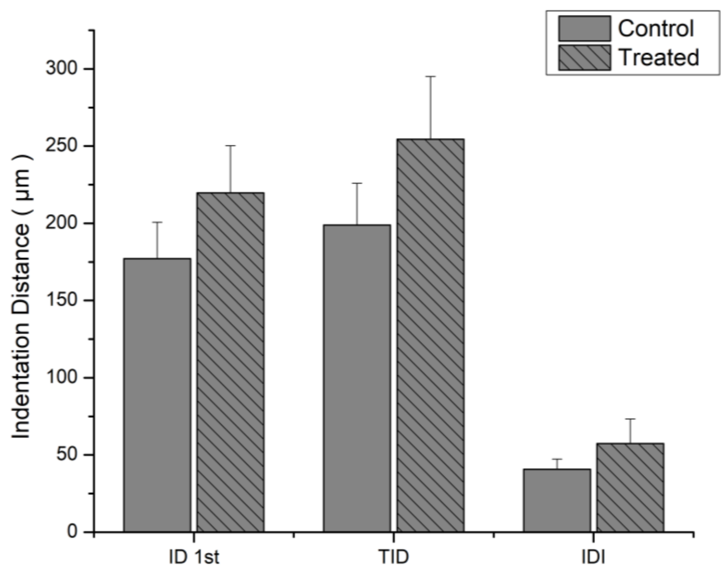

Figure 3.1: Distance RPI parameters of tibia samples

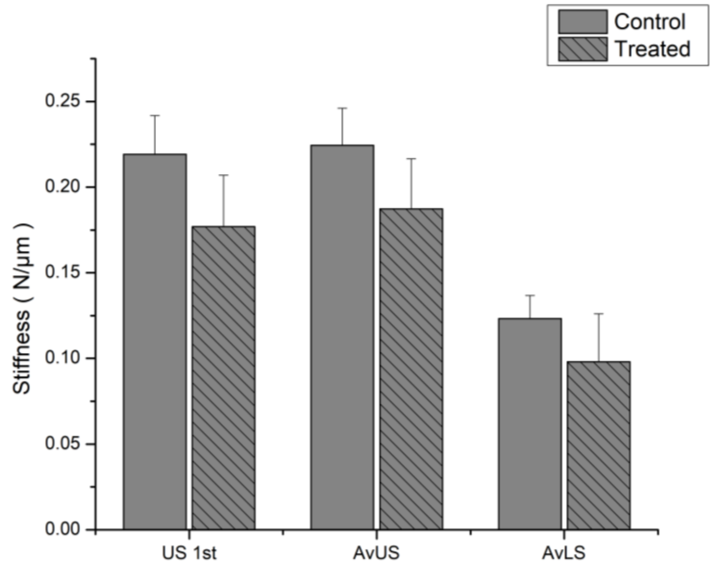

Figure 3.2: Slope RPI Parameters of tibia samples

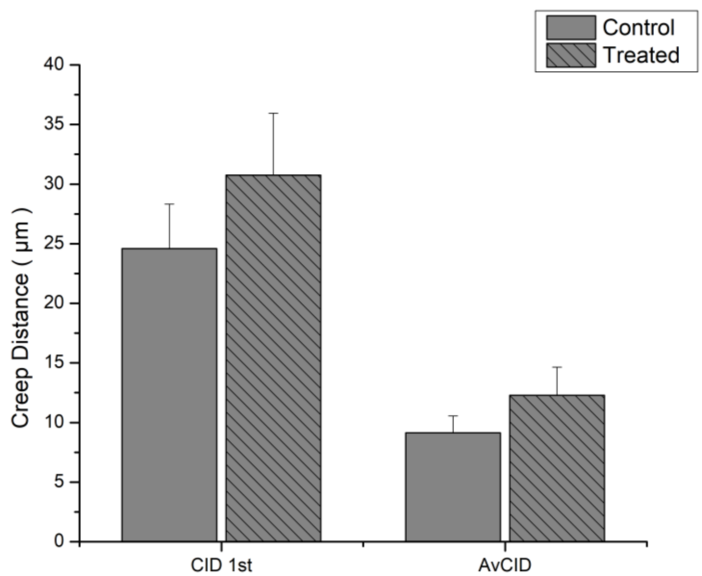

Figure 3.3: Creep RPI Parameters of tibia samples

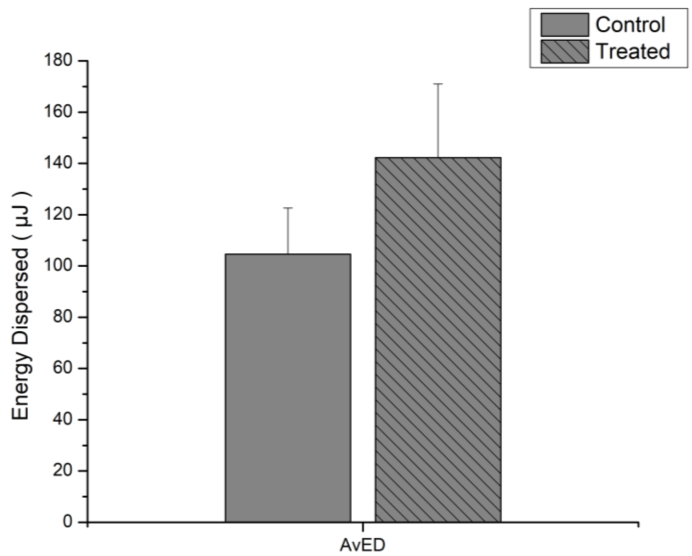

Figure 3.4: Average energy dispersion of tibia samples

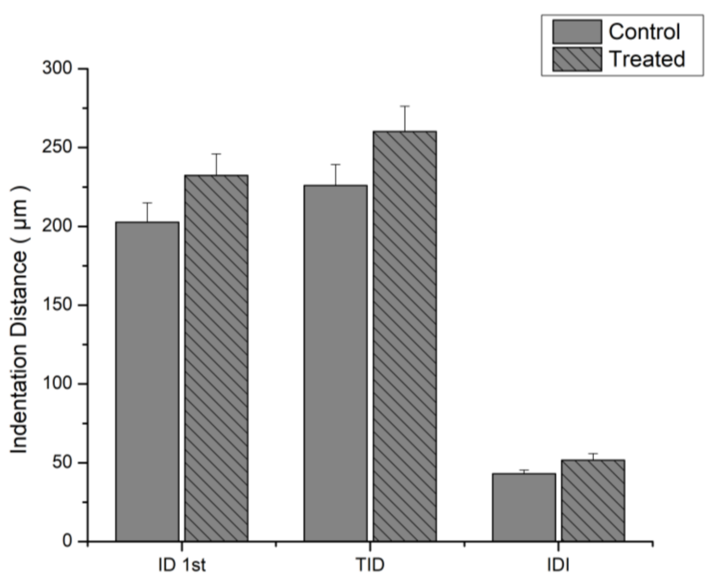

Figure 3.5: Distance RPI parameters of femur samples

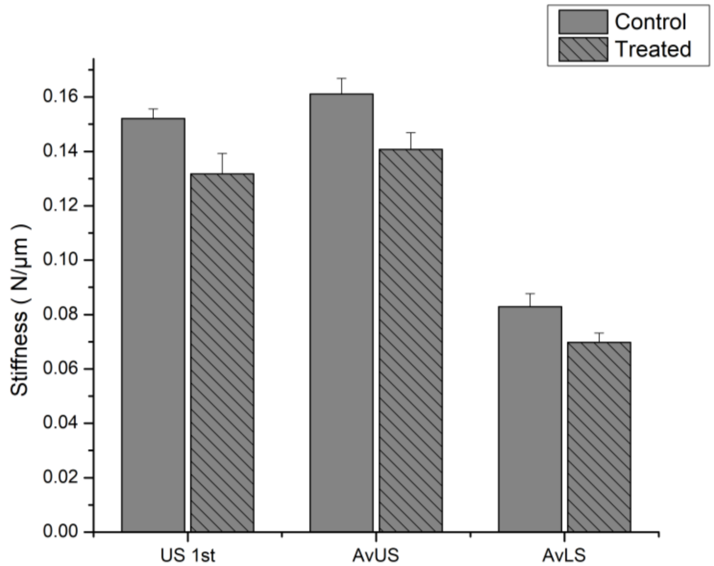

Figure 3.6: Slope RPI parameters of femur samples

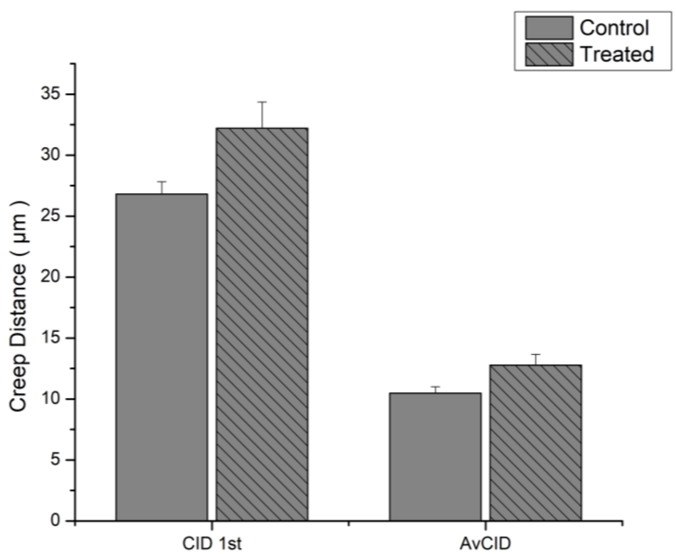

Figure 3.7: Creep RPI parameters of femur samples

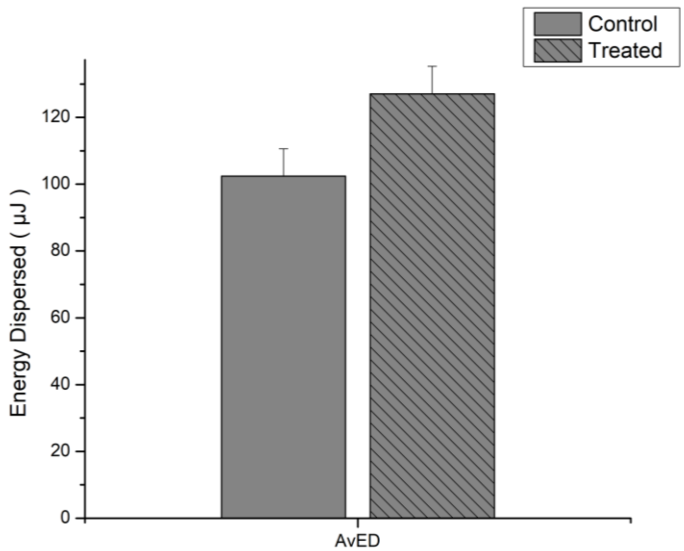

Figure 3.8: Average energy dispersion of femur samples

3.3.3 Compression Results

Two parameters were gathered from compression tests – elastic modulus and ultimate strength. The bone samples underwent linear elastic deformation, and this data was provided by the TestWorks software for each sample. Ultimate stress was taken as the highest stress achieved by the sample. Elastic modulus and ultimate strength comparisons are shown in Figure 3.9. Again, unpaired t-tests assuming unequal means were performed on the data. The differences of means of elastic moduli were shown to be not statistically different. Difference of means of ultimate strength are statistically significant for P = 0.0016.

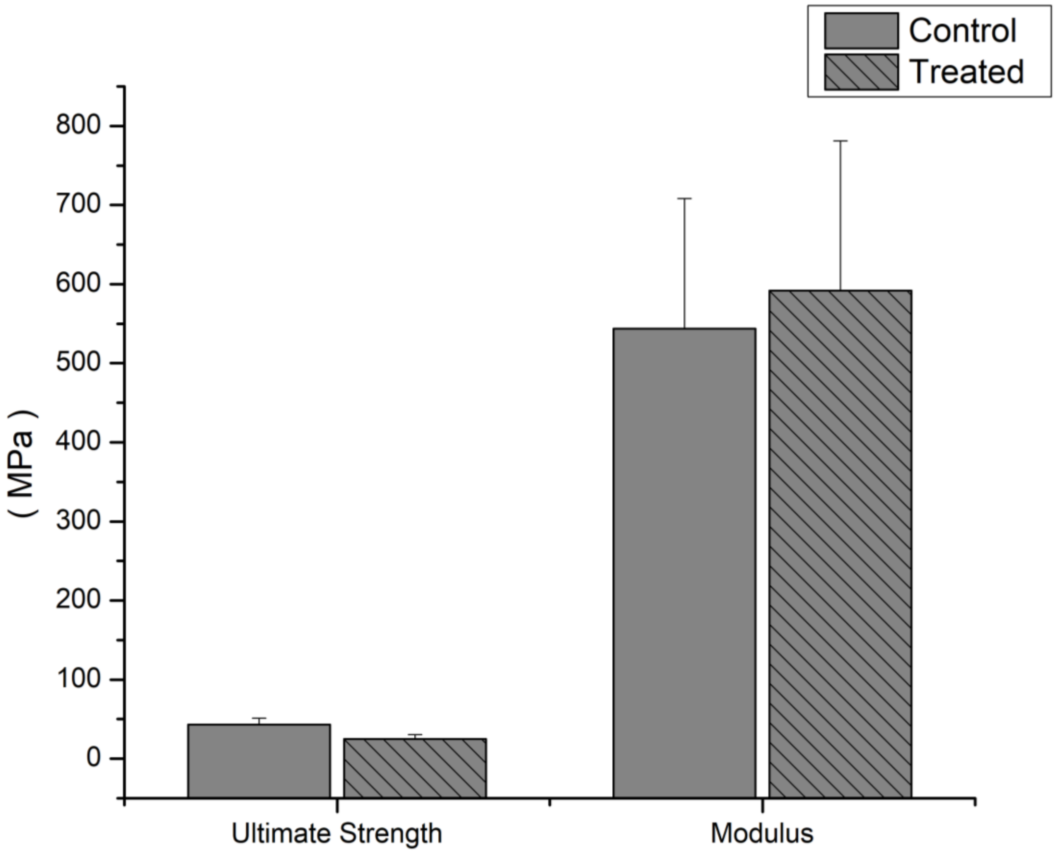

Figure 3.9: Compressive properties of femur samples

3.4 Discussion

3.4.1 Reference Point Indentation

Overall, the RPI parameters support the fact that the induced colitis has an effect of weakening the bones in some way. It is difficult to say in what traditional mechanical sense they are weaker, be it stiffness, fracture toughness, or strength. The nine parameters are in total agreement in all categories. Distance values (Figures 3.1 and 3.5) are overall larger for treated bone. This indicates that the treated bones support less force during plastic deformation, both during first indentation (ID-1st) and subsequent cyclic indentation (IDI and TID). The slope parameters show that there are differences in the elastic portion of the indentation as well – treated samples are less stiff in loading (AvLS) and unloading (AvUS). Creep properties as well, show that under constant load, treated bone will deform further than healthy bone.

It is also valuable to compare the different bone types that were tested. Between femur and tibia tests, trends were identical while specific values are different. This is to be expected however, as the different bones have been shown to have different properties [21].

3.4.2 Compression

Compression results, while much less detailed than the RPI testing, also give insight into mechanical differences caused by induced colitis. Due to the statistically insignificant data, it is difficult to comment on the effect of colitis on stiffness of compression samples. One possible solution to this issue is to use larger dimension samples to test solely for elastic modulus. The hypothesis, however is that stiffness of treated samples would be lower than healthy bone. Ultimate strength results show that the healthy samples are able to support a larger maximum stress on average over the treated bones.

In order to understand further biological changes caused by the induced colitis, results can be separated into quadrants. The medial and anterior quadrants, which in pigs have laminar structure, are in general more mineralized compared to the osteonal posterior and lateral quadrants. This correlates well with the trends displayed in Figure

3.10, which shows that the laminar quadrants of bone of both the control and treated group demonstrate higher ultimate compressive stress when compared to osteonal quadrants. Comparing between the two quadrant types, the difference in ultimate strength is much greater for the treated group than the control group. This may give insight on the mechanism of the decrease of mechanical properties caused by induced colitis.

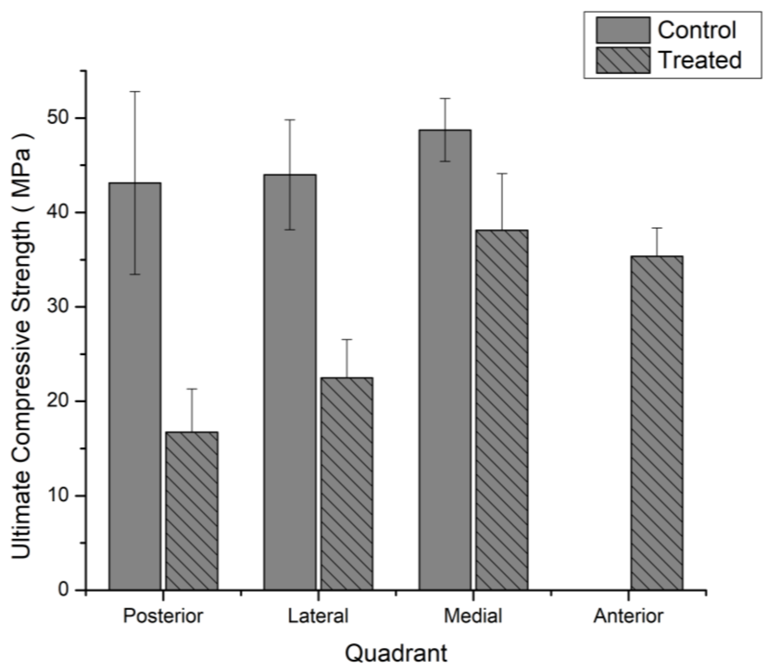

Figure 3.10: Quadrant-separated data of ultimate strength of femur samples

To investigate potential causes for the mechanical differences between treated and control bones, an analysis of porosity and mineralization percentage was carried out. Three samples of each sample group were saturated with DI water and weighed. Samples were then dried at 70°C for 48 hours to evaporate all water in the samples, and then weighed. Dry and wet weights were compared to determine the volume of water, and thus infer the volume of porosity present in each sample. Figure 3.11 shows the porosity values of healthy and colitis sample groups. The difference of means of porosity between sample groups is statistically significant for P = 0.05.

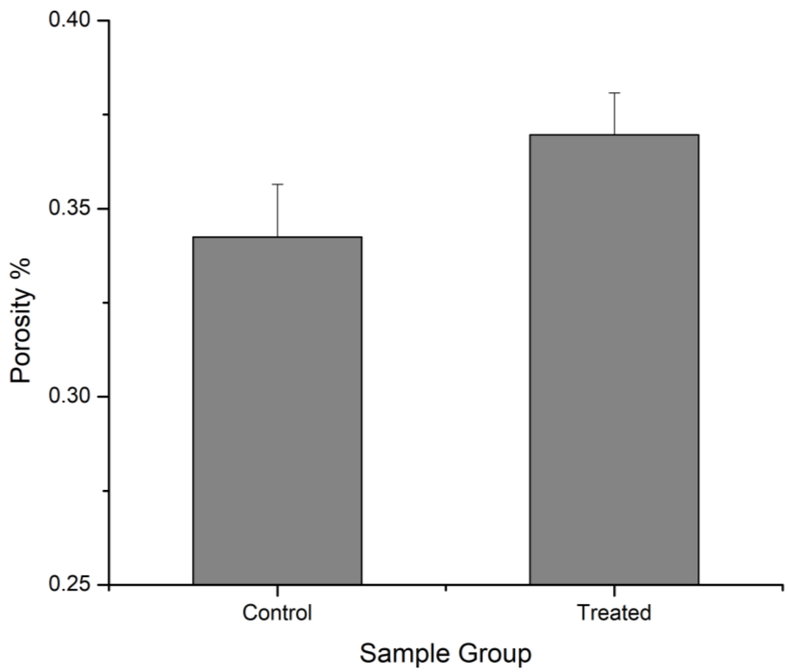

Figure 3.11: Porosity volume percentage of the control and induced-colitis samples

After drying, bone samples were ashed at 800 °C for 18 hours. Ashed weight was then compared to wet weight to determine the weight-percentage of the mineral phase of bone. Figure 3.12 shows the average values per sample. The p value given by an unpaired t-test is 0.0898, indicating that the difference in means is not quite statistically significant.

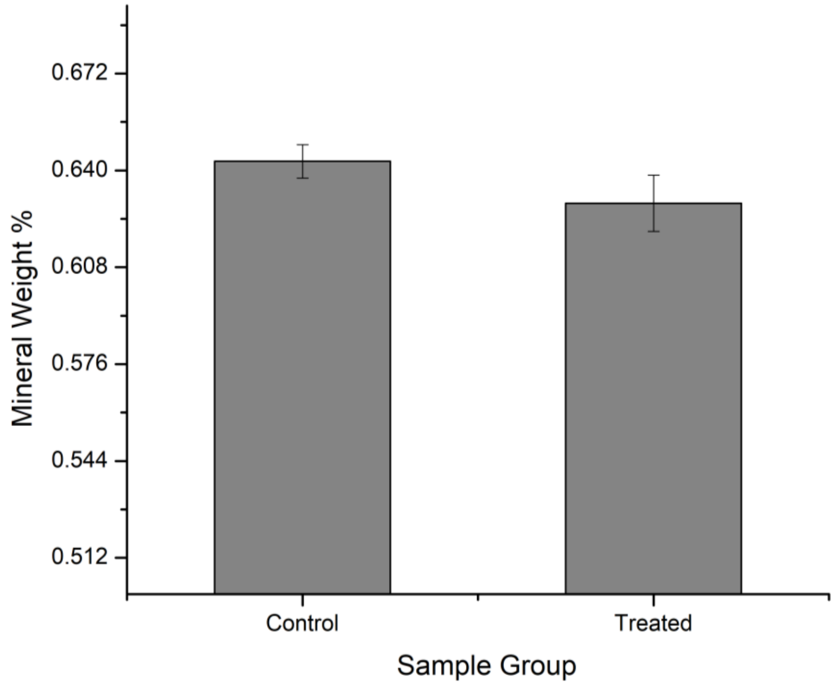

Figure 3.12: Mineral phase weight percentage of the control and induced-colitis samples

3.4.3 Comparing results

Overall, these mechanical tests consistently show that bones under induced colitis are weaker mechanically than healthy bones. The mechanism for this weakening is not well understood, as induced colitis studies are normally focused more on primary intestinal effects, rather than the secondary effects around the body. At this time, the author's best hypothesis for the difference in properties is that the colitis effects that body's ability to absorb and distribute nutrients that are vital for bone development. However, the DSS was only distributed over four days, which is a short time for such drastic differences to occur. This is further supported by the fact that the quadrants containing osteons tend to have lower compressive strength compared to laminar quadrants. More investigation is needed to further understand the relationship between colitis and the effects on bone structure and properties.

When compared to a similar study of induced colitis in piglets, the samples tested in this work are comparable the well-nourished cortical samples, either healthy or colitis-induced [19]. The well-nourished, healthy samples demonstrated a larger energy at fracture than well-nourished colitis samples in 3-point bending, which is consistent with the patterns of ultimate strength demonstrated by the cortical samples tested in this work. Bone area was also demonstrated to be higher in healthy, well-nourished samples, which is consistent with tests performed in this study showing that bone volume is higher in control samples.

3.5 Conclusions

In conclusion, reference point indentation and compression tests were performed on bones with laboratory induced colitis to determine differences in properties from healthy bones. Between both tests, bones that were treated to induce the disease showed differences in properties that imply that they were mechanically weaker.

Chapter 4: Quantitative Backscatter Imaging of Developing Pig Cortical Bone

4.1 Introduction

4.1.1 Introduction to Bone

Many medically relevant properties of bone can be determined by the level of mineralization present in bone tissue. Bone mineralization can be affected by factors including age, location in bone [22], and disease [23 - 25]. Mineralization can also be used as an input to finite element analysis (FEA) to predict bone strength or fragility [26, 27].

Hydroxyapatite, chemical formula $Ca_5(PO_4)_3(OH)$, is the main mineral component of bone. By weight, hydroxyapatite is 39.86% calcium. It is distributed in bone as crystals of mineral interwoven with the collagen matrix present in bone. This phase of bone can be isolated for mechanical experimentation using an ashing method or by using chemical treatment. Mineralization can also be investigated directly in ex-vivo or in-vivo samples using a variety of imaging techniques.

4.1.2 Introduction to Imaging Techniques

There are many methods of determining bone quality. According to Compston, bone quality can be separated into the following categories: microarchitecture, mineralization microdamage, and matrix and mineral composition [28]. Many clinical imaging methods, such as micro-CT and MRI, are useful for investigation of bone microarchitecture in live patients. However, deeper investigation on microstructure and mineralization is possible using microscopy techniques on ex-vivo bone samples.

Specifically, electron microscopy is a method with excellent resolution capabilities; up to single-digit nanometers resolution is possible under ideal conditions of biological samples [29]. When using an electron microscope, there are several choices of technique to determine sample composition. The most popular choices are energy-dispersive x-ray spectroscopy (EDS) and quantitative backscattered electron imaging (QBEI).

Compared to EDS, QBEI is a quick method to determine mineralization. To process a comparable area to the images presented in this work, it would take multiple hours to perform an elemental analysis. This is a viable method to explore an unknown composition or multiple elements at once. However, when investigating a single, known compound, QBEI is advantageous in time spent and equipment needed.

QBEI is has been performed extensively on trabecular bone of various species [24, 25]. Microscopy of any sort on trabecular bone is challenging due to the necessity to imbed the sample in resin.

The goal of the study is two-fold. The first goal is to develop a sample preparation method and understand the QBEI data analysis technique for use with bone samples. Next, the effect of age on the calcium mineralization of pig bone will be examined using the proposed technique.

4.2 Materials and Methods

4.2.1 Sample Preparation

Samples were cut from the mid-diaphysis of pig femurs to a thickness of approximately 2 mm. Small thickness is crucial when preparing samples to reduce excess charge buildup on samples. Animals' diet and genetics were controlled to be identical for a separate study.

Femur samples were polished according to a standard procedure, using the following series of polishing grits: 200, 400, 800, 1200, 2000, 4000. A combination of alumina powder of 100 μm, 25 μm, and 5 μm radii, and cloth disks were used to polish samples further. A procedure for fixation and drying was performed to make the samples suitable to placea vacuum environment. This consisted of the following steps: 24 hours of hydrogen peroxide to remove loose soft tissue; 24 hours of SEM fixative; 2 hours each of 10%, 50%, 95%, and three times 100% ethanol solution. The samples were then dried completely using critical point drying.

To prepare for SEM imaging, samples were mounted on sample pins using carbon tape. To increase surface visibility, the femur samples and elemental standards were initially coated in approximately 50 angstroms of carbon. Further carbon coating was applied as needed to reduce charge build up in some samples. To encourage charge to flow away from the sample surfaces, silver paint was applied to the sides of the bone samples to form an electrical connection to the sample pins.

4.2.2 Scanning Electron Microscopy Settings

A FEI Quanta FEG 450 SEM was used to image the bone samples. To perform backscatter electron imaging, an Everhart-Thornley detector was affixed to the column of the SEM. Images were taken at a working distance of approximately 10 mm, acceleration voltage of 20 kV, and spot size of 4.

4.2.3 Data Analysis

To account for varying contrast and brightness of the backscatter electron image, a set of elemental standards must be used. For this work, a pin containing the following four compounds was obtained: aluminum (Al), calcium carbonate ($CaCO_3$), silicon dioxide (SiO_2), and magnesium oxide (MgO). The effective atomic number, or Z-number, can be calculated by weighted average of the elemental make-up of each standard, according to the following formula, presented in Roschger [30]:

$$Z_{eff} = \frac{\sum N_i * A_i * Z_i}{\sum N_i * A_i},$$

in which N_i represents the amount of each atom, A_i represents the atomic weight of each atom, and Z_i represents the atomic number of each atom.

Table 4.1 shows the calculated effective Z-number of the elemental standards and pure hydroxyapatite.

Table 4.1: Effective atomic numbers of standard compounds

Compound	Chemical Formula	Z_{eff}
Hydroxyapatite	$Ca_5(PO_4)_3(OH)$	14.06
Aluminum	Al	13.00
Calcite	CaCO3	12.57
Quartz	SiO2	10.80
Magnesium Oxide	MgO	10.41

By capturing backscatter electron images of each standard, one can calibrate for differing brightness and contrast settings. Once the average grey level of each standard is determined, one can plot grey level versus effective atomic number. Shown in Figure 4.1, an example plot of grey level versus compound effective Z-number is demonstrated. A linear relationship between the two variables is expected regardless of imaging settings.

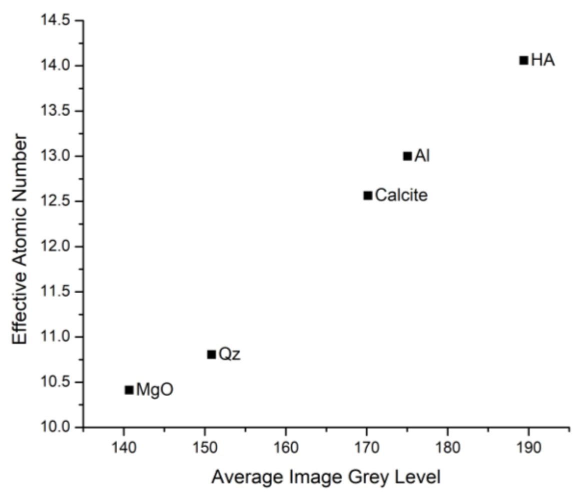

Figure 4.1: Example plot of standard compound grey level against effective atomic number

To convert grey level to calcium weight-percentage, we equate the Z_{eff} value of hydroxyapatite (14.06) to the calcium weight percentage of hydroxyapatite (39.86%). For a second point of linear fit, zero grey level is equated to zero calcium weight-percentage. This method of linear fitting causes inaccuracies at very low calcium weight-percentages. However, the samples explored in this work are expected to have mineralization levels far outside of this error-prone region.

To determine calcium mineralization of the bone samples, several backscatter images were taken of each quadrant of bone (medial, lateral, anterior, and posterior).

The mean and standard deviation of each backscatter image can be determined in a multitude of ways. For this study, ImageJ was used to create histograms of the distribution of grey levels. Thresholding of extreme high and low grey values also may be necessary. For this work, grey values outside of 30 to 225 are excluded.

Using the correlation of grey level to calcium mineralization discussed above, one can calculate the average calcium mineralization of each image. Alternatively, a mapping of calcium mineralization can be applied on a per-pixel basis, but that is not performed here.

4.3 Results

4.3.1 Age Effect Results

Here, mineralization percentage of five different ages is graphed. Figure 4.2 plots the mineralization of each age. Figure 4.3 displays a zoomed view of the same data. Table 4.2 shows the number of images taken per sample group.

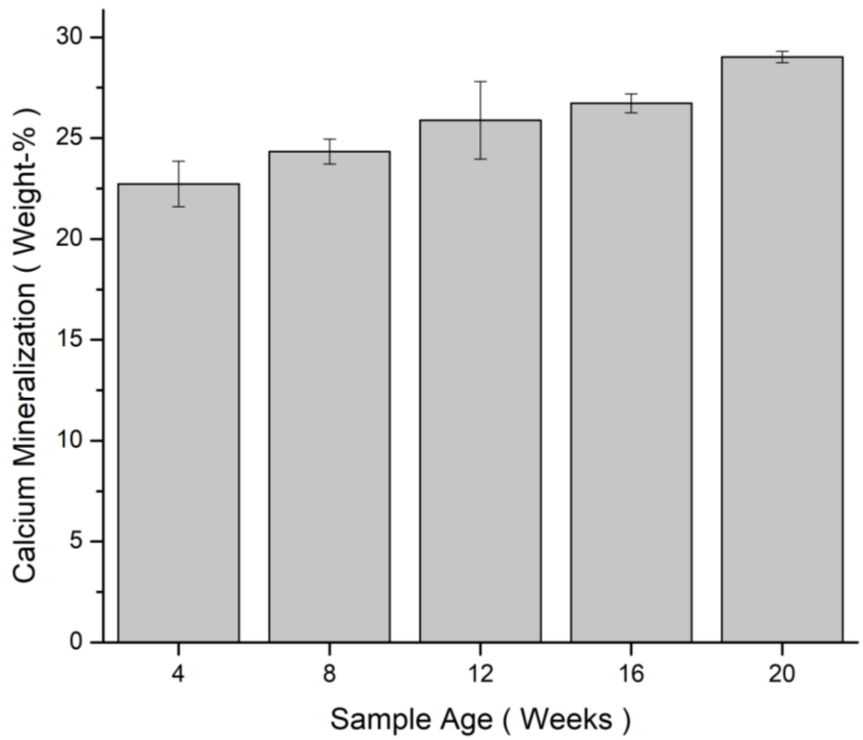

Figure 4.2: Plot of calcium weight-percentage of the five age groups

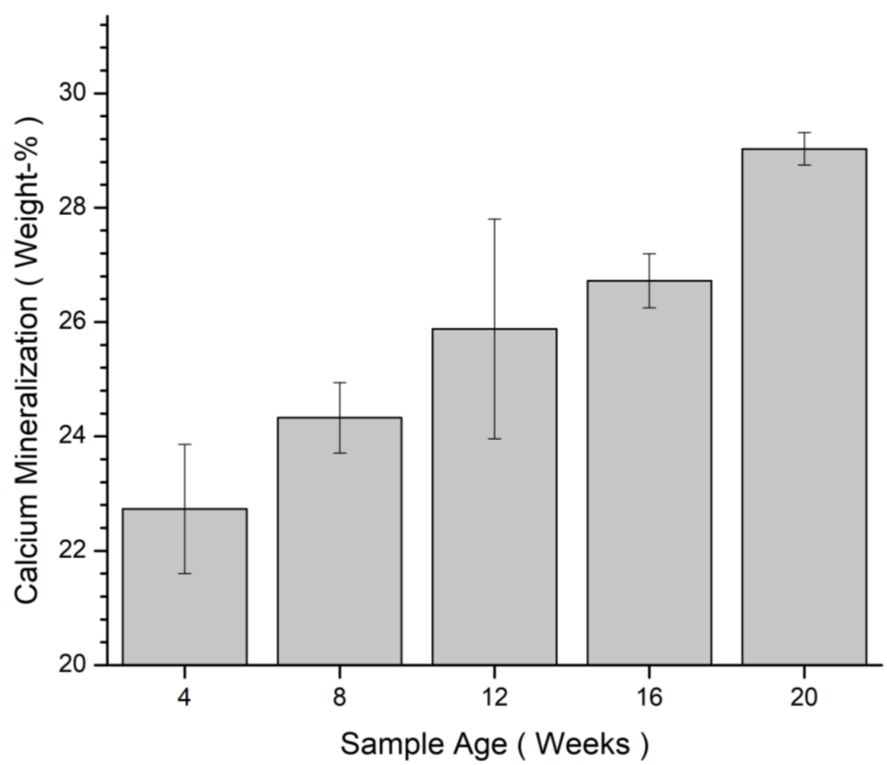

Figure 4.3: Plot of calcium weight-percentage of the five age groups (zoomed)

Table 4.2: Number of images taken per age

Age	Images Captured
4	30
8	23
12	27
16	36
20	20

Mean mineralization percentage of each age was compared using unpaired t-tests. The mean mineralization percentage of each age is statistically different ($p < 0.05$), except for 12 weeks. This large variation in the 12-week sample group is most likely due to sample charging causing grey level variation in the images. Otherwise, most means are very significantly ($p < 0.0001$) different.

4.3.2 Bone Quadrant Results

Each age can be separated further into quadrant data. Here, some quadrants are not presented due to sample charging issues. Quadrant separated mineralization data is shown in Figures 4.4 through 4.8.

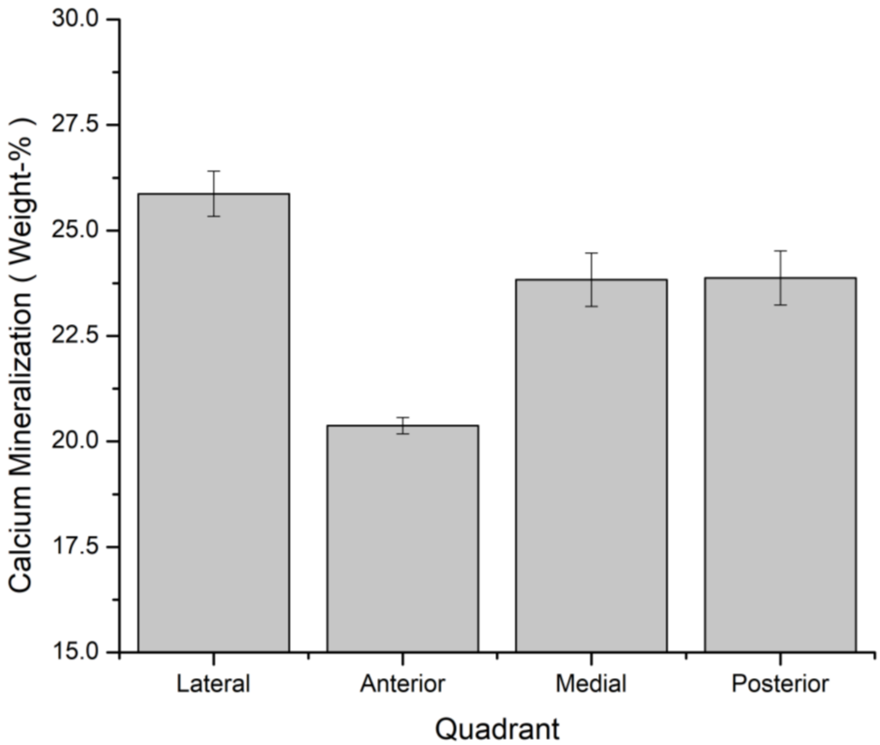

Figure 4.4: Quadrant-separated calcium weight-percentage data for four-week-old sample

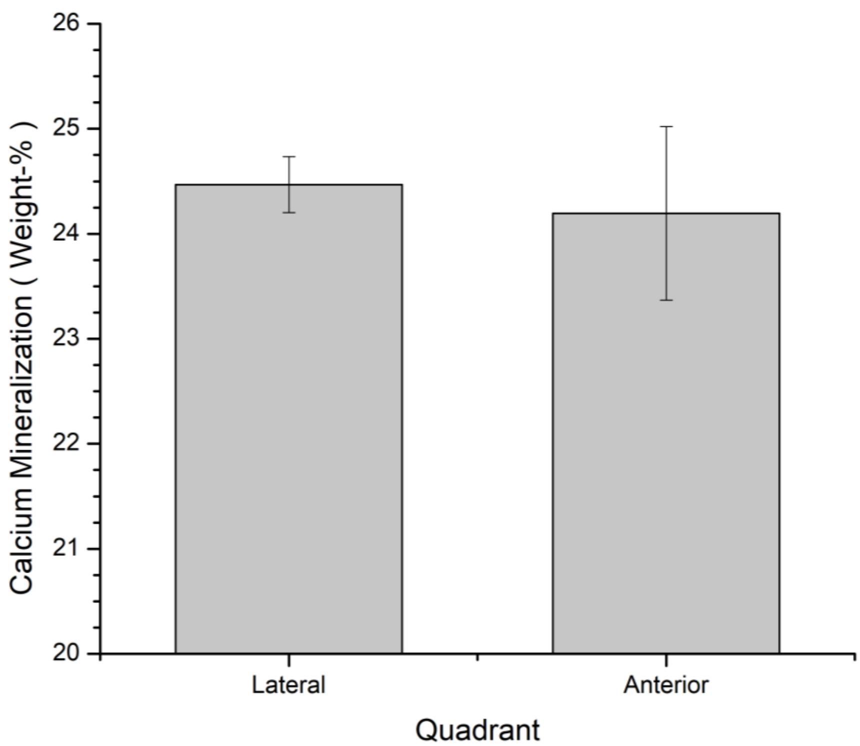

Figure 4.5: Quadrant-separated calcium weight-percentage data for eight-week-old sample

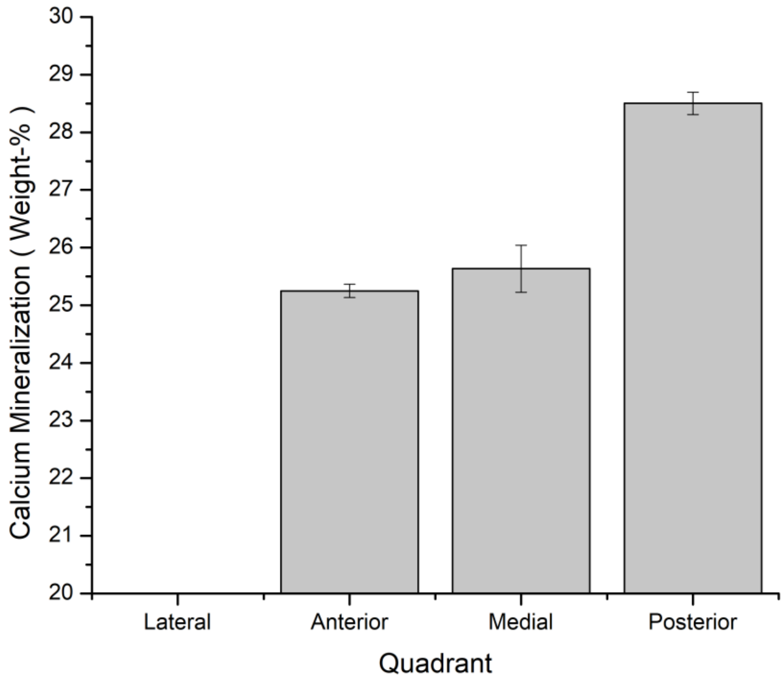

Figure 4.6: Quadrant-separated calcium weight-percentage data for twelve-week-old sample

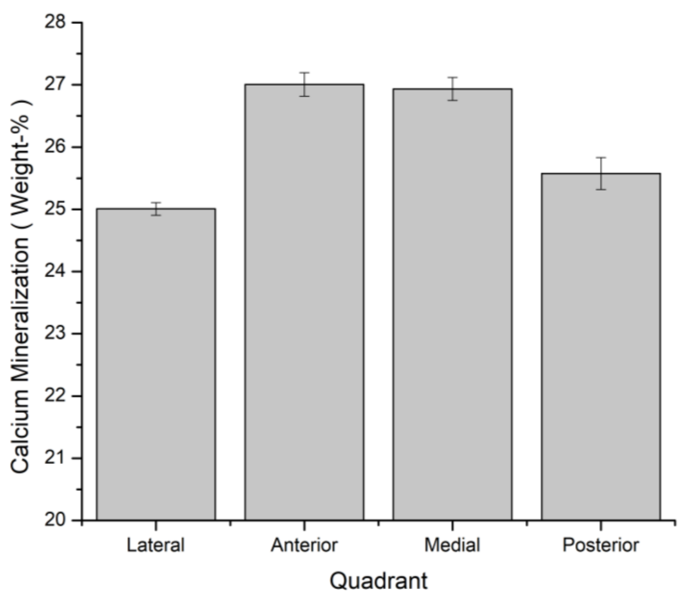

Figure 4.7: Quadrant-separated calcium weight-percentage data for sixteen-week-old sample

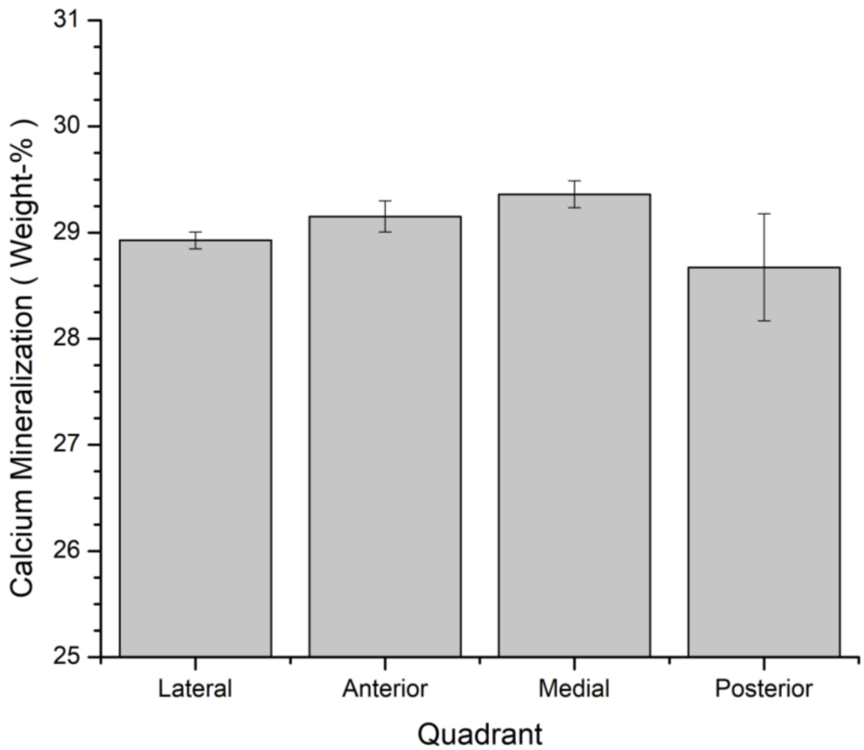

Figure 4.8: Quadrant-separated calcium weight-percentage data for twenty-week-old sample

4.4 Discussion

4.4.1 Age Effect Discussion

Age data displays an expected trend in terms of calcium mineralization. The increase of calcium mineralization is roughly linear with age. Figures 4.2 and 4.3 of the age data show this linear trend well, and the linear fit of the data is very high, with R^2 value of 0.9835. The relationship is decreased somewhat by the large variation of the 12-week sample image group. This variation could have been decreased by changing several factors; to decrease the amount of sample charging, the sample could have been cut thinner, had thicker carbon coating prior to imaging, or lowered accelerating voltage during imaging.

Bone is generally accepted to be composed of about 60% inorganic mineral phase by weight [31]. In order to convert the data presented, calcium weight percentage, to bulk mineralization, a simple factor can be applied. By dividing by the percentage of calcium by weight in hydroxyapatite (0.3986), calcium weight-percentage can be converted to bulk hydroxyapatite. Figure 4.9 plots bulk mineralization weight-percentage by age. As shown, the hydroxyapatite weight-percentage is around the predicted proportion.

These age-related changes in mineralization correlate well with the BMSi measurements discussed in Chapter 2, as well as nanoDMA measurements that will be discussed in the next chapter. Because mineralization is a partial factor in the mechanical properties of bone, it can be inferred from these QBEI measurements that the mineralization increases from age at least a partial cause for the increase in mechanical properties of the studied bone.

4.4.2 Bone Quadrant Discussion

When separating mineralization data into quadrants, two trends emerge. Firstly, one can observe that for very young bone, there is no clear trend with regard to quadrants. For older samples, however, distinctions between quadrants are apparent.

Observing Figures 4.4 through 4.6, younger bones have very little correlation between the quadrant the image was captured and mean mineralization percentage. However, Figures 4.7 and 4.8 show a pattern of two quadrants having significantly higher mean mineralization compared to the other quadrants. The quadrants with higher values, the anterior and medial quadrants, are lamellar quadrants in pig. Lamellar quadrants contain little to no osteons. Because osteons are far less mineralized than interstitial bone, the osteonal quadrants on average have significantly lower mineral content. Figure 4.9 shows an example image of an osteonal region of bone, which displays the extreme difference in contrast between the osteon and interstitial bone.

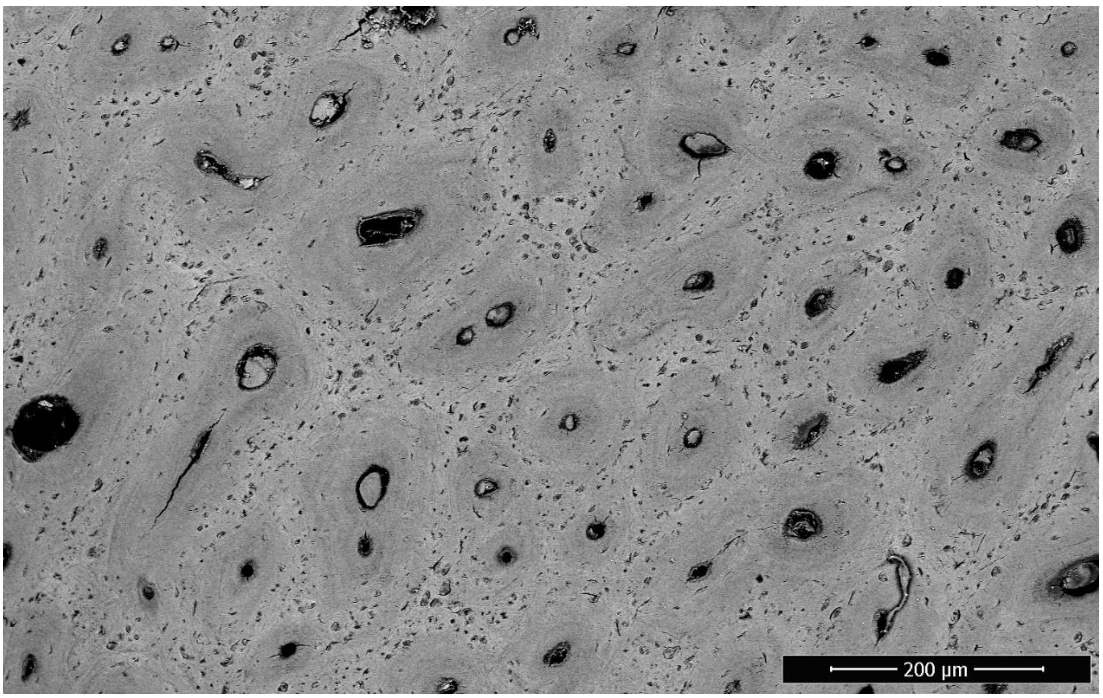

Figure 4.9: Example of backscatter image of osteonal bone

Observing the quadrant separated compression data shown previously in Figure 3.10, the mineralization measurements are in agreement. Due to the lower mineralization of osteonal quadrants, the ultimate strength of bone was shown to be lower. This effect was amplified when observing the induced-colitis samples, where the nutritional problems created a further loss of mineral in the bone tissue.

4.4.3 Limitations of Study

The limitations of this study are mostly problems in sample preparation. Some quadrants, as well as the entire 0-week sample, are missing data due to excessive sample charging, which produces grey level variation that is unrelated to mineralization.

The use of QBSE imaging is also useful in conjunction with localized measurement techniques, such as nanoindentation, Raman spectroscopy, and others. Further application of QBSE in combination with the proposed methods would be a relevant extension of this work and would lead to further understanding of the age-related changes in young pig bone.

4.5 Conclusions

In this work, quantitative backscatter electron imaging was used to determine the calcium mineralization of developing porcine femur. The methodology of data processing using known elemental standards to calibrate image variation in electron microscopy imaging was explained. By using this calibration method, one can adjust contrast and brightness settings of the SEM image and still be able to compare values taken at different sessions with possibly different values.

To demonstrate this methodology, five age groups; 4, 8, 12, 16, and 20 weeks old; of pig femora were imaged along with the elemental standards. QBSE imaging shows that the calcium mineralization of the whole bone increases approximately linearly as age increases. Statistical analysis of the data demonstrates that the mean mineralization of the imaged regions of each sample are significantly different than other ages, disregarding the 12-week sample group. The 12-week sample group experienced moderate sample charging that created large data variation. All other age groups' mean mineralization are significantly different. By separating each age into quadrant data, new trends emerge. The laminar quadrants of bone, the anterior and medial sections, are much less mineralized than the posterior and lateral quadrants due to fewer osteons present in laminar bone. This trend does not appear in young bone, however. The younger samples show no correlation between quadrant type and calcium mineralization percentage.

Chapter 5: Nanoindentation of Periosteum of Developing Pig Cortical Bone

5.1 Introduction

5.1.1 Introduction to Nanoindentation of Bone

One of the defining characteristics of biological tissue, especially bone, is variation of mechanical properties at small scales due to complex microstructure [31]. Due to the interwoven collagen and mineral phases of bone, mechanical tests can often have large error based on microstructure of particular samples. This is evident in the compression data presented in Chapter 3, which has large error in the elastic properties measured. However, because bone is a composite of collagen (polymer) and mineral phase (ceramic), it behaves as a viscoelastic material.

A particularly common method of measuring viscoelastic material properties is dynamic mechanical analysis, or DMA. DMA has previously been performed on large-scale samples of bone to determine viscoelastic parameters. [32 - 35]. However, it is impossible to measure local variation of properties caused by microstructure using macroscale methods such as compression testing or DMA.

Nanoindentation, a method that is capable of probing, has been performed on bone to determine microscale mechanical property variations [36 - 38]. However, most studies using nanoindentation focus on quasistatic properties, particularly modulus and hardness. NanoDMA allows for microscale testing of viscoelastic properties on large scale samples, while being able to average over multiple indents to mitigate property variations caused by microstructure.

5.1.2 Motivation

The reference point indentation (RPI) technique is a novel method of directly measuring the mechanical properties of bone in an in-vivo or diagnostic environment. However, both currently available RPI devices, the BioDent and Osteoprobe, only indent to a depth of approximately 100 microns at maximum. This region, known as the periosteal portion of bone, near the outside of the bone is constantly reforming in living tissue, and can have drastically different microstructure, and thus properties, compared to the bulk of the material [31]. Furthermore, RPI parameters have been previously shown to be disproportionally affected by variations of surface microstructure when compared to the whole-bone scale [10].

As discussed in Chapter 2, one of the major goals of research of RPI is to link the measurements done by these devices to traditional mechanical terms. Due to the small size of the indentation region, milling or sawing out a sample of periosteal bone large enough to perform macroscale mechanical tests would be difficult. Thus, nanoDMA is an ideal method to understand the differences between periosteal bone tissue and the bulk, or endosteal tissue.

5.2 Materials and Methods

5.2.1 Sample Preparation

Pig tibiae were cut into ring samples at the mid-diaphysis from samples aged 4-weeks-old and 16-weeks-old. To reduce sample variability, animals were taken from the same genetic line and given the same diet. Sample thickness was not crucial to control, but ensuring that samples were thick enough such that the indentation surface is above the rim of a petri dish makes the indentation process much easier.

Samples were polished using the standard procedure for imaging or indentation. Paper grits of 200, 400, 800, 1200, 2000, and 4000 were used, followed by alumina powder polishing of 100 μm, 25 μm, and 5 μm radii. Polishing samples helps to reduce variability in measurements by ensuring that the indenter tip is always indenting on a relatively flat surface and avoiding edge effects.

Polished samples were then fixed to a petri dish using Crystalbond 509. The petri dish is held in place in the nanoindenter using a vacuum stage. NanoDMA was performed on the Hysitron TI-950 Triboindenter in the Frederick Seitz Materials Research Laboratory Central Research Facilities, University of Illinois.

5.2.2 Indentation Parameters

To select indentation regions for each quadrant, sample boundaries were created using the TriboScan software. Periosteal regions were created within the first 100 microns from the edge of the samples on each quadrant. Endosteal sample regions were placed near the middle of the sample, measured radially.

To perform dynamic indentations, a nanoDMA transducer was used, equipped with a Berkovich tip. To calibrate the transducer, an air calibration was performed for both the indentation axis and DMA frequency generation. Stage calibration was performed using an H-pattern on aluminum. To determine the tip area function, a quasi-static partial unload indentation was performed on quartz. Based on this indentation profile, the tip area function was calculated using the modified Oliver-Pharr Method.

To perform indentation, samples were loaded to 4000 μN over 5 seconds. Then, a randomized frequency sweep was applied. Frequencies from 10 Hz to 200 Hz were tested in intervals of 10 Hz. The frequencies for 60 Hz, 120 Hz, and 180 Hz had to be adjusted to 61.5 Hz, 121.5 Hz, and 181.5 Hz to avoid resonance of the transducer. After all frequencies have been tested, samples were unloaded over 5 seconds. This indentation process was repeated five times spaced 10 μm apart for periosteal and endosteal locations for each quadrant of the two sample ages. The complex modulus, hardness, and tan-delta measurement of the five indentations were averaged and recorded.

5.3 Results

Due to the large number of figures, the full set of plots can be found in Appendix A. In Figures A.1 through A.8, the magnitude of complex modulus is plotted against indentation frequency for endosteal bone and periosteal bone. From the 4-week-old sample, all quadrants except the posterior quadrant show overlap between endosteal and periosteal bone.

Figures A.9 through A.16 show plots of hardness versus dynamic frequency. Hardness was captured as a measure of quasi-static mechanical properties of each tissue location. Of all quadrant and ages, only the four-week-old anterior indentations have similar hardness values between the tested locations.

Plots showing tan-delta versus dynamic frequency are shown in Figures A.17 to A.24. All quadrants demonstrate no significant difference of measurement from varying frequency or indentation location. The tan-delta measurement for all indentation locations are roughly equal at 0.2. The tan-delta value is presented as a measure of the viscous damping of the material.

5.4 Discussion

5.4.1 Discussion of Trends

As discussed previously, the only location to have similar hardness values between periosteal and endosteal bone is the anterior quadrant on the 4-week-old sample. All other locations have differences between the two radial locations. When comparing the 4-week-old and 16-week-old measurements, the magnitude of the difference between the two locations is larger in the older bones. From this, we can assume that endosteal bone is more difficult to induce damage on. Also, hardness measurements show very minor variation from changes in indentation frequency.

Of the quadrants of the four-week-old sample, only one quadrant has significantly different values of complex modulus. However, this trend is not present in the older sample. This shows that endosteal region in older tissue is significantly stiffer. However, because complex modulus is comprised of storage and loss moduli, it is not possible to state which property is affecting the difference between the tissue locations with this measurement alone. Similar to the hardness measurements, there is very minor variation of complex modulus with respect to measurement frequency, but not enough to call statistically significant.

When comparing tan-delta measurements between endosteal and periosteal regions of both tested ages, the two regions' measurements are approximately equal within the measured error. Furthermore, all measured locations have approximately equal measurements of tan-delta, ranging from 0.1 to 0.2. Knowing the definition of the tan-delta measurement, we can assume that bone tissue has an equal ratio of viscous loss to elastic storage for all the tested quadrants, frequencies, and radial locations.

Combining this result with the knowledge that the magnitude of complex modulus is most often greater in endosteal bone, one can infer that the reason for this is that the storage modulus is greater in the region. This can be verified by examining the storage modulus directly as well. Knowing this, we can conclude that the quasi-static mechanical parameters, hardness and elastic modulus, are most likely different between endosteal and periosteal bone tissue.

5.4.2 Implications for RPI Testing

From the three measured parameters discussed above, one can conclude that the quasistatic mechanical properties of endosteal and periosteal bone tissue are different under the tested samples. In both ages tested, the hardness value is different for all quadrants. For the older test sample, elastic modulus is also higher in endosteal bone.

These differences in mechanical properties between the outer and inner layer of bone have a potential to make significant effects on some of the measurement parameters unique to RPI. When considering the BioDent, the parameters that are measured consist of both quasi-static (loading and unloading slopes, first indentation distance), creep parameters, and energy parameters. Due to the similarity of viscous loss between the endosteal and periosteal regions, the creep parameters are likely comparable between the regions. However, the quasi-static parameters such as the slope parameters and first indentation parameters are predicted to be different.

Given these findings, RPI is unlikely to be able to determine bulk quasistatic properties directly. This is not necessarily a negative, but when using RPI to test, it must be considered that the thin periosteal layer of bone will have differing properties compared to the rest of the bone. It is possible to make predictions based on further correlation between periosteal and endosteal bone, if such a connection exists.

Limitations of Study

The first notable limitation of this study is that the indentation direction not the same orientation that reference point indentation is generally performed at. Due to the microstructure of bone, the orientation of the indent likely will change the measured values. However, it is hard to predict whether the trend between periosteal and endosteal regions would change based on orientation.

The second limitation is based on experimental parameters. As discussed above, there was little to no variation of any of the parameters caused by indentation frequency. Testing higher frequencies may result in frequency response of the tissue. It is also difficult to determine how properties change with age with only two differently aged samples. More age groups would also help to determine when in the animal's lifetime the age-related changes occur.

5.5 Conclusions

In conclusion, nanoDMA was used to determine the differences between the inner (endosteal) and outer (periosteal) regions of porcine bone. The three parameters presented were hardness, magnitude of complex modulus, and tan-delta, or the ratio of loss and storage moduli. Data was separated into two ages, 4-week-old and 16-week-old, and by quadrants of bone. This separation of endosteal and periosteal measurement was motivated by understanding if the measurements done via reference point indentation could directly probe the bulk mechanical properties of bone.

The quasi-static properties of bone, namely hardness and storage modulus, were shown to have significant differences when comparing endosteal and periosteal regions of the older sample group. The 4-week-old sample had only significantly different measurement of hardness. However, almost all quadrants of both ages have equal tan-delta measurements between both regions of interest. This shows that the viscous loss of bone tissue is roughly equal throughout the entire bone. The implication for RPI is such that one must be aware of possible differences between quasistatic properties of the inner and outer layers of bone while interpreting results. However, RPI parameters that measure the time-dependent nature of bone are applicable for the entire tissue, rather than just the outer layer.

Chapter 6: General Summary

Several methods of characterization were applied to developing pig bone throughout this thesis. Among them were reference point indentation using BioDent and Osteoprobe, compression testing, nano-dynamic mechanical analysis, and quantitative backscatter electron imaging. Many of the age and location related trends of bone tissue were detected and collaborated between each measurement method. Thus, this work stands as a promising start into the cataloging of mechanical changes present in developing bone.

The brief study of the Osteoprobe shows that BMSi increases with age from zero weeks old to 20 weeks old. The increase in BMSi seems to decrease for older ages, so there is a potential for the measurements to even out at some point. Further investigation with older ages is necessary to determine if this is the case.

Bone treated to induce colitis was also tested against control bone of the same age. Both compression tests and BioDent RPI measurements conclude that the mechanical properties of the treated sample are significantly lowered. To understand why that is the case, a group of samples were ashed to determine porosity and mineral content. Both parameters measured lower in treated samples, but only porosity measurements show statistical significance. More samples are required to determine if the mineral content measurement is significant, but following the mechanical measurements it is expected to be.

Calcium mineralization was measured in the zero to twenty-week-old samples using quantitative backscatter electron imaging. This connects to both the Osteoprobe measurements and nanoDMA measurements as a way to verify that mechanical property changes are at least partially caused by these mineralization increases. Mineralization was shown to increase linearly with age, and to be lower in osteonal quadrants (posterior and lateral). The variation of mineralization in quadrants is demonstrated both using QBEI as well as in the compression data.

Finally, viscoelastic properties of the inner and outer regions of bone were measured in two ages of bone. This is motivated by the fact that reference point indentation is limited to testing the outermost 100 microns of bone, and that properties between this thin layer and the bulk tissue may be different. It was determined that the viscous loss of bone was approximately equal within the tested frequencies and ages. However, the elastic modulus and hardness was shown to be potentially different between the two tested ages. This has implications with regards to RPI testing, but does not discredit the technique. One must be aware of these potential differences when interpreting results from reference point indentation. Further testing in higher frequencies and different ages is necessary for understanding this trend more clearly.

In conclusion, several factors of variation within bone were studied. The several measurement techniques largely complimented each other and verified trends that occurred. While this thesis covers several different causes of variation within bone, there are several situations that can be studied using the discussed techniques. Due to the complexity of bone as a biological material, understanding the changes of it as a material is a very open-ended and vast region of study.

References

[1] Hansma, P. K., Turner, P. J., & Fantner, G. E. (2006). Bone diagnostic instrument I. *Review of Scientific Instruments*, *77*(7), 1–6. https://doi.org/10.1063/1.2221506

[2] Diez-Perez, A., Güerri, R., Nogues, X., Cáceres, E., Peña, M. J., Mellibovsky, L., … Hansma, P. K. (2010). Microindentation for in vivo measurement of bone tissue mechanical properties in humans. *Journal of Bone and Mineral Research : The Official Journal of the American Society for Bone and Mineral Research*, *25*(8), 1877–1885. https://doi.org/10.1002/jbmr.73

[3] Kaye, B., Randall, C., Walsh, D., & Hansma, P. (2012). The Effects of Freezing on the Mechanical Properties of Bone. *The Open Bone Journal*, (805), 14–19.

[4] Hansma, P., Turner, P., Drake, B., Yurtsev, E., Proctor, A., Mathews, P., … Kohn, D. (2008). Bone diagnostic instrument II: Indentation distance increase. *Review of Scientific Instruments*, *79*(6), 1–8. https://doi.org/10.1063/1.2937199

[5] Randall, C., Mathews, P., Yurtsev, E., Sahar, N., Kohn, D., & Hansma, P. (2009). Bone diagnostic instrument III: Testing mouse femora. *Review of Scientific Instruments*, *80*(6), 2–4. https://doi.org/10.1063/1.3147383

[6] Setters, A., & Jasiuk, I. (2014). Towards a standardized reference point indentation testing procedure. *Journal of the Mechanical Behavior of Biomedical Materials*, *34*, 57–65. https://doi.org/10.1016/j.jmbbm.2014.01.012

[7] Jenkins, T., Coutts, L. V., Dunlop, D. G., Oreffo, R. O. C., Cooper, C., Harvey, N. C., & Thurner, P. J. (2015). Variability in reference point microindentation and recommendations for testing cortical bone: Maximum load, sample orientation, mode of use, sample preparation and measurement spacing. *Journal of the Mechanical Behavior of Biomedical Materials*, *42*, 311–324. https://doi.org/10.1016/j.jmbbm.2014.09.030

[8] Randall, C., Bridges, D., Guerri, R., Nogues, X., Puig, L., Torres, E., … Hansma, P. K. (2013). Applications of a New Handheld Reference Point Indentation Instrument Measuring Bone Material Strength. *Journal of Medical Devices*, *7*(4), 410051–410056. https://doi.org/10.1115/1.4024829

[9] Lescun, T. B., Hoffseth, K., Yang, H. T., Hansma, P. K., Kopeikin, H. S., & Chandrasekar, S. (2016). Effect of various testing conditions on results for a

handheld reference point indentation instrument in horses. *American Journal of Veterinary Research*, *77*(1), 39–49.

[10] Krege, J. B., Aref, M. W., McNerny, E., Wallace, J. M., Organ, J. M., & Allen, M. R. (2016). Reference point indentation is insufficient for detecting alterations in traditional mechanical properties of bone under common experimental conditions. *Bone*, *87*, 97–101. https://doi.org/10.1016/j.bone.2016.04.002

[11] Hoffseth, K., Randall, C., Hansma, P., & Yang, H. T. Y. (2015). Study of indentation of a sample equine bone using finite element simulation and single cycle reference point indentation. *Journal of the Mechanical Behavior of Biomedical Materials*, *42*, 282–291. https://doi.org/10.1016/j.jmbbm.2014.11.020

[12] Idkaidek, A., Agarwal, V., & Jasiuk, I. (2017). Finite element simulation of Reference Point Indentation on bone. *Journal of the Mechanical Behavior of Biomedical Materials*, *65*, 574–583. https://doi.org/10.1016/j.jmbbm.2016.08.031

[13] Javaid, M. K., & Cooper, C. (2002). Prenatal and childhood influences on osteoporosis. *Best Practice and Research: Clinical Endocrinology and Metabolism*, *16*(2), 349–367. https://doi.org/10.1053/beem.2002.0199

[14] Lamb, E. J., Wong, T., Smith, D. J., Psonà, D. E. S. I. M., Leyà, A. J. C., Moniz, C., & Uller, A. F. M. (2002). Metabolic bone disease is present at diagnosis in patients with inflammatory bowel disease. *Alimentary Pharmacology and Therapeutics*, 1895–1902. https://doi.org/10.1046/j.0269-2813.2002.01363.x

[15] Mandair, G. S., & Morris, M. D. (2015). Contributions of Raman spectroscopy to the understanding of bone strength. *BoneKEy Reports*, *4*(January), 1–8. https://doi.org/10.1038/bonekey.2014.115

[16] Michalak, A., Mosi??ska, P., & Fichna, J. (2016). Common links between metabolic syndrome and inflammatory bowel disease: Current overview and future perspectives. *Pharmacological Reports*, *68*(4), 837–846. https://doi.org/10.1016/j.pharep.2016.04.016

[17] Bowden, L. S., Jones, C. J., & Ryan, S. W. (1999). Bone mineralisation in ex-preterm infants aged 8 years. *European Journal of Pediatrics*, *158*(8), 658–661. https://doi.org/10.1007/s004310051171

[18] Brennan, A.-M., Murphy, B. P., & Kiely, M. E. (2016). Optimising preterm nutrition: present and future. *Proceedings of the Nutrition Society*, *75*(2), 154–161. https://doi.org/10.1017/S0029665116000136

[19] Vassilyadi, P., Harding, S. V., Hazell, T. J., Weiler, H. A., & Wykes, L. J. (2016). Colitis, independent of macronutrient intake, compromises bone structure and strength in growing piglets. *Pediatric Research*, *80*(5), 753–758. https://doi.org/10.1038/pr.2016.135

[20] Young, D., Ibuki, M., Nakamori, T., Fan, M., & Mine, Y. (2012). Soy-derived di- and tripeptides alleviate colon and ileum inflammation in pigs with dextran sodium sulfate-induced colitis. *The Journal of Nutrition*, *142*(2), 363–368. https://doi.org/10.3945/jn.111.149104

[21] Hamed, E., Lee, Y., & Jasiuk, I. (2010). Multiscale modeling of elastic properties of cortical bone. *Acta Mechanica*, *213*(1–2), 131–154. https://doi.org/10.1007/s00707-010-0326-5

[22] Bouxsein, M. L., & Seeman, E. (2009). Quantifying the material and structural determinants of bone strength. *Best Practice and Research: Clinical Rheumatology*, *23*(6), 741–753. https://doi.org/10.1016/j.berh.2009.09.008

[23] Tjhia, C. K., Odvina, C. V., Rao, D. S., Stover, S. M., Wang, X., & Fyhrie, D. P. (2011). Mechanical property and tissue mineral density differences among severely suppressed bone turnover (SSBT) patients, osteoporotic patients, and normal subjects. *Bone*, *49*(6), 1279–1289. https://doi.org/10.1016/j.bone.2011.09.042

[24] Misof, B. M., Paschalis, E. P., Blouin, S., Fratzl-Zelman, N., Klaushofer, K., & Roschger, P. (2010). Effects of 1 year of daily teriparatide treatment on iliacal bone mineralization density distribution (BMDD) in postmenopausal osteoporotic women previously treated with alendronate or risedronate. *Journal of Bone and Mineral Research*, *25*(11), 2297–2303. https://doi.org/10.1002/jbmr.198

[25] Roschger, P., Dempster, D. W., Zhou, H., Paschalis, E. P., Silverberg, S. J., Shane, E., … Klaushofer, K. (2007). New observations on bone quality in mild primary hyperparathyroidism as determined by quantitative backscattered electron imaging. *Journal of Bone and Mineral Research : The Official Journal of the American Society for Bone and Mineral Research*, *22*(5), 717–723. https://doi.org/10.1359/JBMR.070120

[26] Hirata, Y., Inaba, Y., Kobayashi, N., Ike, H., Fujimaki, H., & Saito, T. (2013). Comparison of mechanical stress and change in bone mineral density between two types of femoral implant using finite element analysis. *Journal of Arthroplasty*, *28*(10), 1731–1735. https://doi.org/10.1016/j.arth.2013.04.034

[27] Langton, C. M., Pisharody, S., & Keyak, J. H. (2009). Comparison of 3D finite element analysis derived stiffness and BMD to determine the failure load of the excised proximal femur. *Medical Engineering and Physics*, *31*(6), 668–672. https://doi.org/10.1016/j.medengphy.2008.12.007

[28] Compston, J. (2006). Bone quality: what is it and how is it measured? *Arquivos Brasileiros de Endocrinologia E Metabologia*, *50*(4), 579–585. https://doi.org/S0004-27302006000400003 [pii]

[29] Hermann, R., & Mller, M. (1991). High resolution biological scanning electron microscopy: A comparative study of low temperature metal coating techniques. *Journal of Electron Microscopy Technique*, *18*(4), 440–449. https://doi.org/10.1002/jemt.1060180414

[30] Roschger, P., Roschger, P., Fratzl, P., Fratzl, P., Eschberger, J., Eschberger, J., … Klaushofer, K. (1998). Validation of Quantitative Backscattered Electron Imaging for the Measurement of Mineral Density Distribution in Human Bone Biopsies. *Bone*, *23*(4), 319–326.

[31] Bonney, H., Colston, B. J., & Goodman, a. M. (2011). Regional variation in the mechanical properties of cortical bone from the porcine femur. *Medical Engineering and Physics*, *33*(4), 513–520. https://doi.org/10.1016/j.medengphy.2010.12.002

[32] Yamashita, J., Furman, B. R., Rawls, H. R., Wang, X., & Agrawal, C. M. (2001). The use of dynamic mechanical analysis to assess the viscoelastic properties of human cortical bone. *Journal of Biomedical Materials Research*, *58*(1), 47–53. https://doi.org/10.1002/1097-4636(2001)58:1<47::AID-JBM70>3.0.CO;2-U

[33] Yeni, Y. N., Shaffer, R. R., Baker, K. C., Dong, N., Grimm, M. J., Les, C. M., Fyhrie, D. P., (2001). The effect of yield damage on the viscoelastic properties of cortical bone tissue as measured by dynamic mechanical analysis. *Journal of Biomedical Materials Research – Part A*, 82 (3), 530–537

[34] Abdel-Wahab, A. A., Alam, K., & Silberschmidt, V. V. (2011). Analysis of anisotropic viscoelastoplastic properties of cortical bone tissues. *Journal of the*

Mechanical Behavior of Biomedical Materials, *4*(5), 807–820. https://doi.org/10.1016/j.jmbbm.2010.10.001

[35] Grover, K., Lin, L., Hu, M., Muir, J., & Qin, Y. X. (2016). Spatial distribution and remodeling of elastic modulus of bone in micro-regime as prediction of early stage osteoporosis. *Journal of Biomechanics*, *49*(2), 161–166. https://doi.org/10.1016/j.jbiomech.2015.11.052

[36] Donnelly, E., Boskey, A. L., Baker, S. P., & van der Meulen, M. C. H. (2009). Effects of tissue age on bone tissue material composition and nanomechanical properties in the rat cortex. *Journal of Biomedical Materials Research Part A*, *9999A*, NA-NA. https://doi.org/10.1002/jbm.a.32442

[37] Kim, D. G., Haghighi, A., Kwon, H. J., Coogan, J. S., Nicolella, D. P., Johnson, T. B., … Agnew, A. M. (2017). Sex dependent mechanical properties of the human mandibular condyle. *Journal of the Mechanical Behavior of Biomedical Materials*, *71*(February), 184–191. https://doi.org/10.1016/j.jmbbm.2017.03.012

[38] Sun, J., Wu, W., Xue, W., Tong, J., & Liu, X. (2016). Anisotropic nanomechanical properties of bovine horn using modulus mapping. *IET Nanobiotechnology*, *10*(5), 334–339. https://doi.org/file:///C:/Users/igorz/Downloads/07577911.pdf

Appendix A: Complete Set of nanoDMA Figures

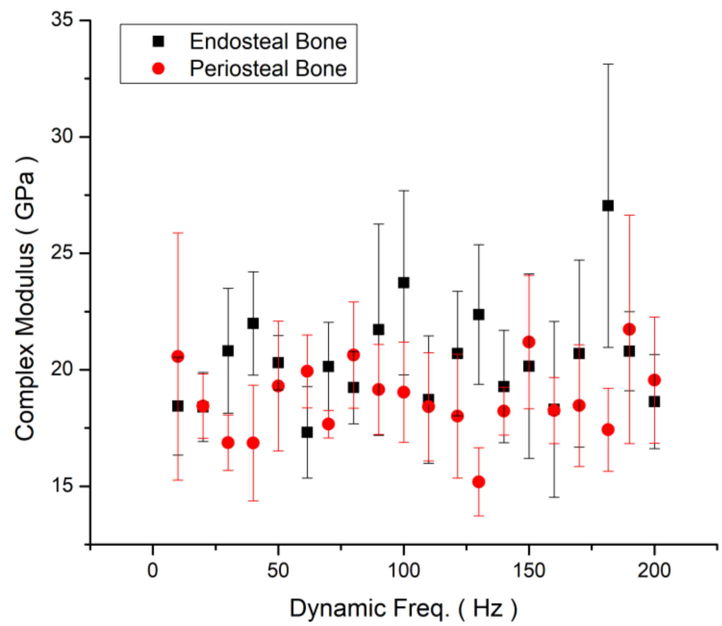

Figure A.1: Complex modulus - anterior quadrant of 4-week-old bone

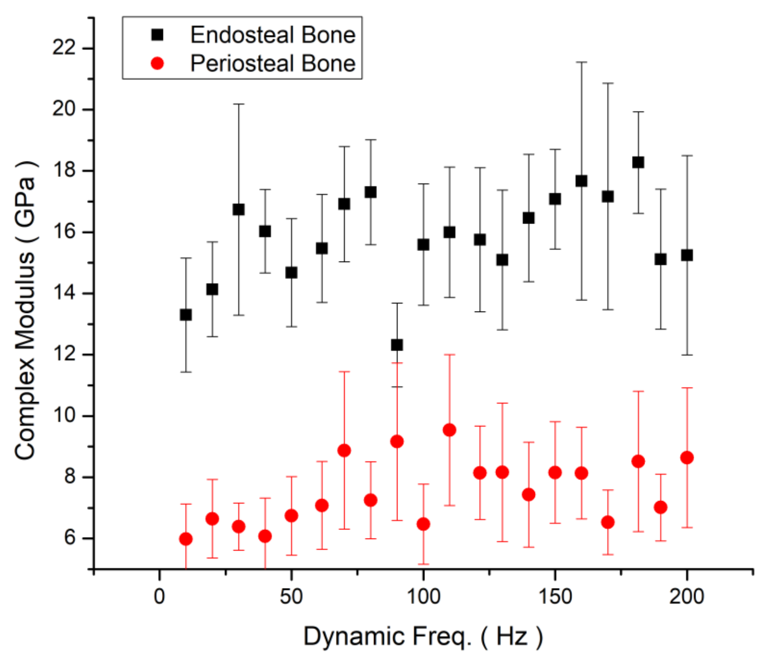

Figure A.2: Complex modulus - lateral quadrant of 4-week-old bone

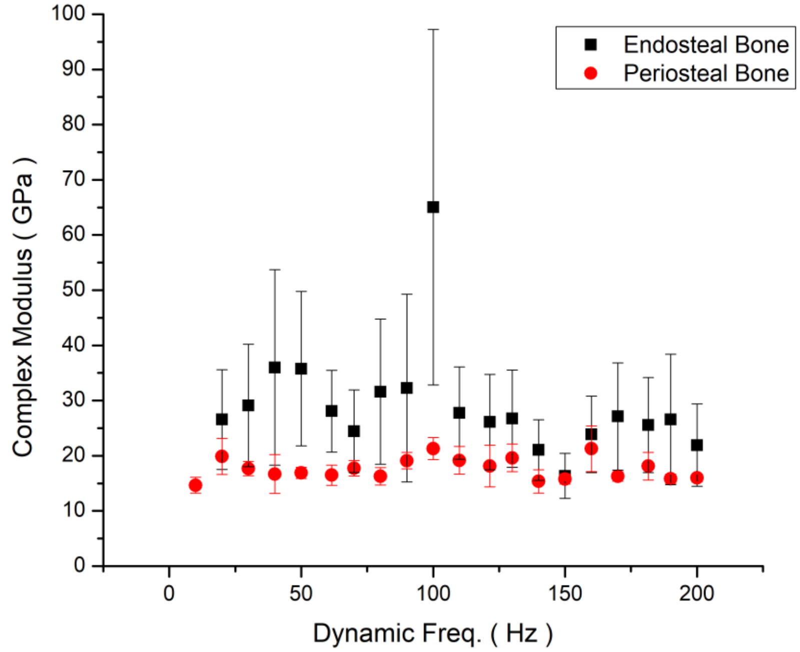

Figure A.3: Complex modulus - medial quadrant of 4-week-old bone

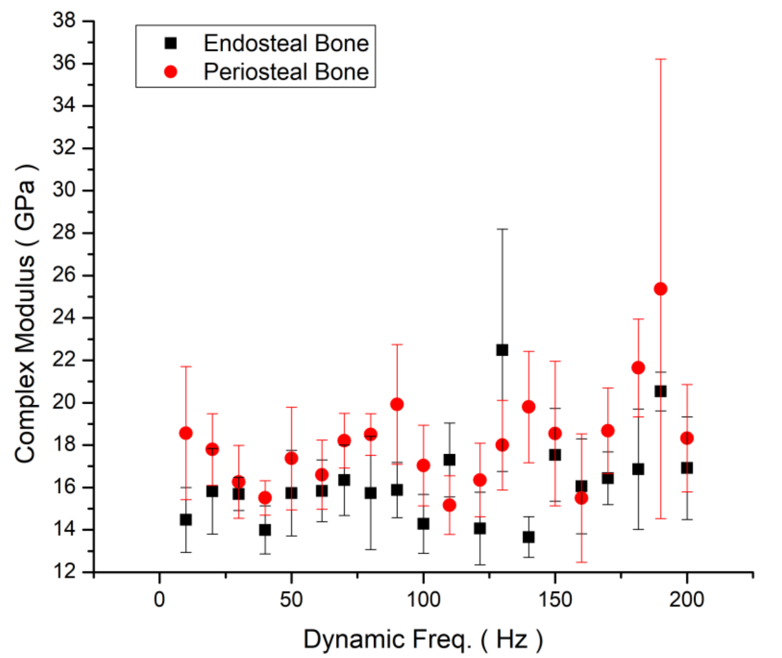

Figure A.4: Complex modulus - posterior quadrant of 4-week-old bone

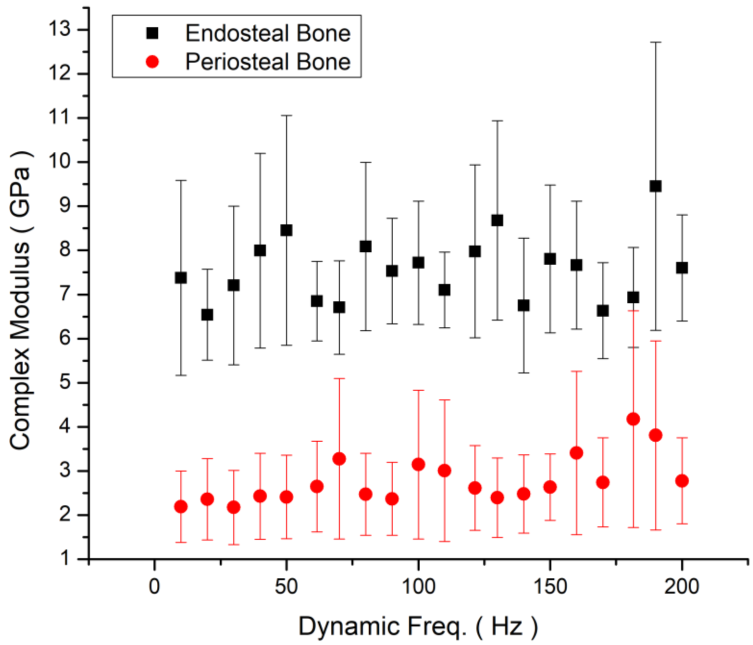

Figure A.5: Complex modulus - anterior quadrant of 16-week-old bone

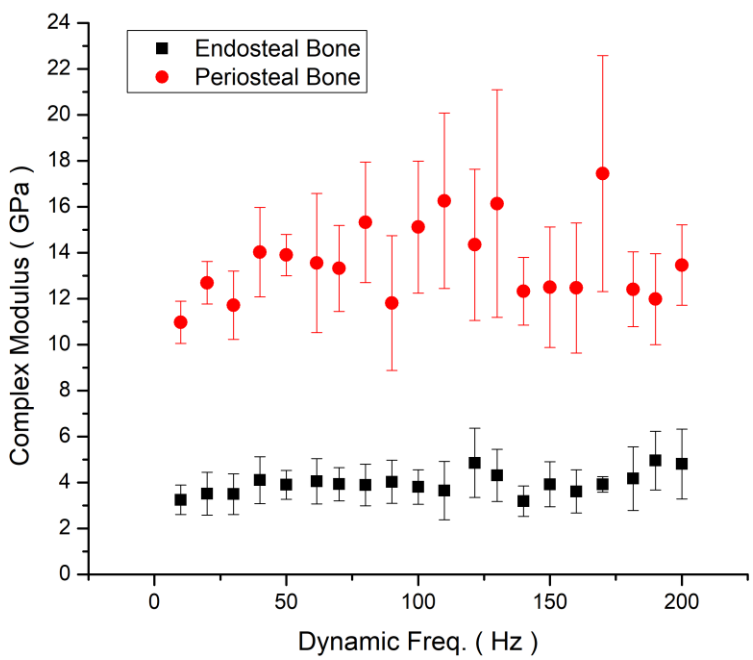

Figure A.6: Complex modulus - lateral quadrant of 16-week-old bone

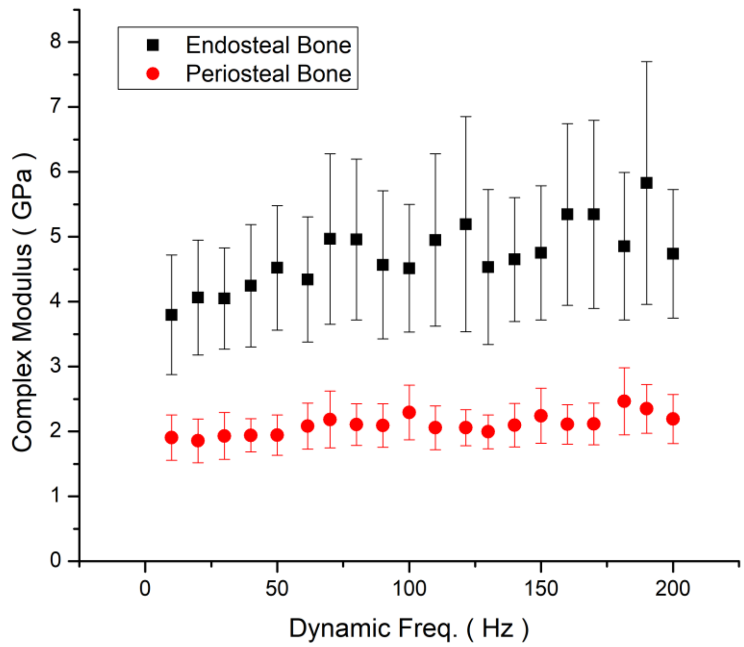

Figure A.7: Complex modulus - medial quadrant of 16-week-old bone

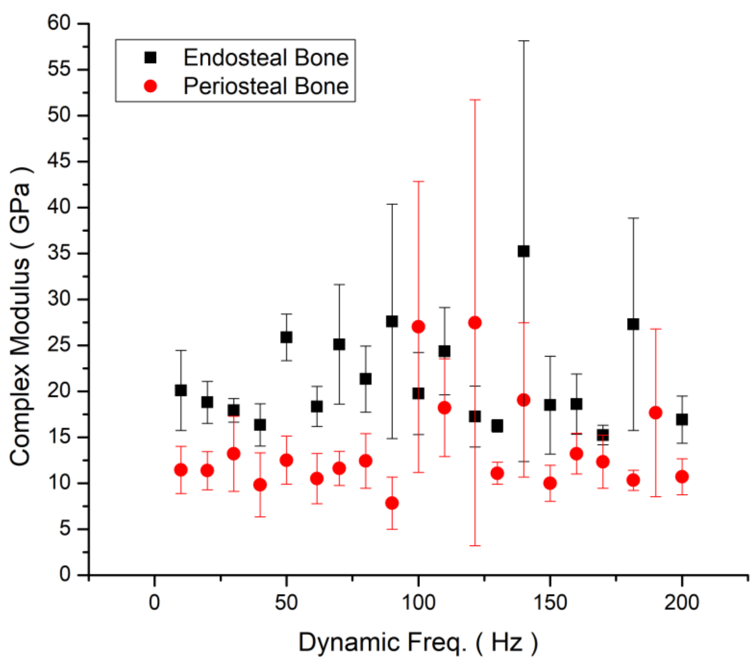

Figure A.8: Complex modulus - posterior quadrant of 16-week-old bone

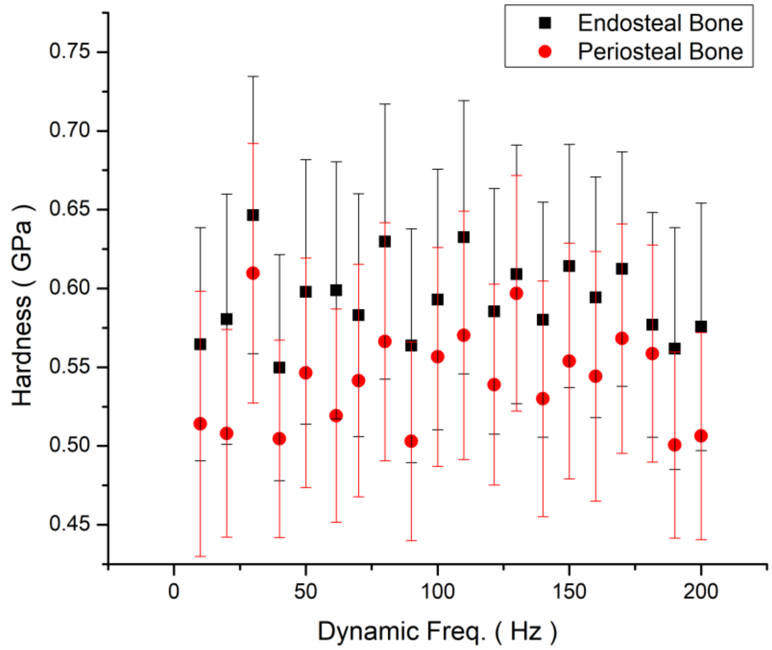

Figure A.9: Hardness - anterior quadrant of 4-week-old bone

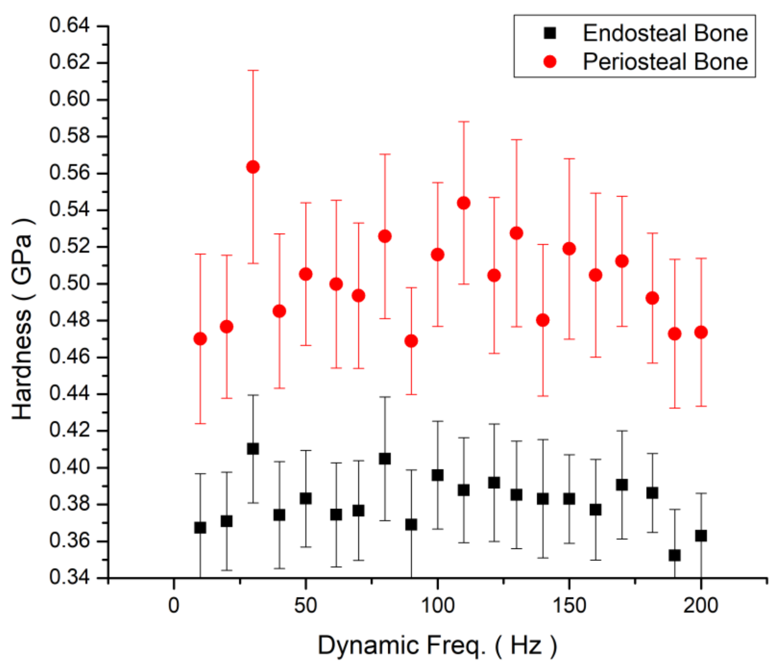

Figure A.10: Hardness - lateral quadrant of 4-week-old bone

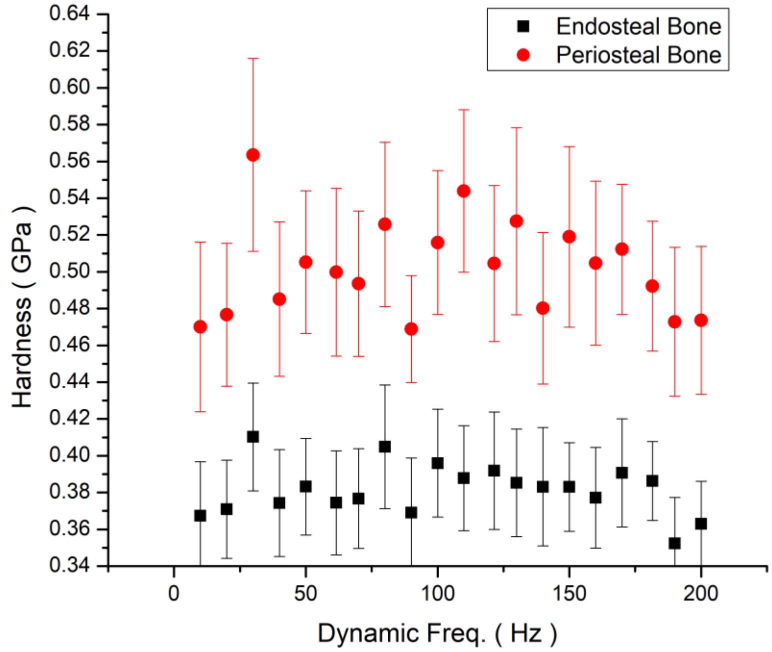

Figure A.11: Hardness - medial quadrant of 4-week-old bone

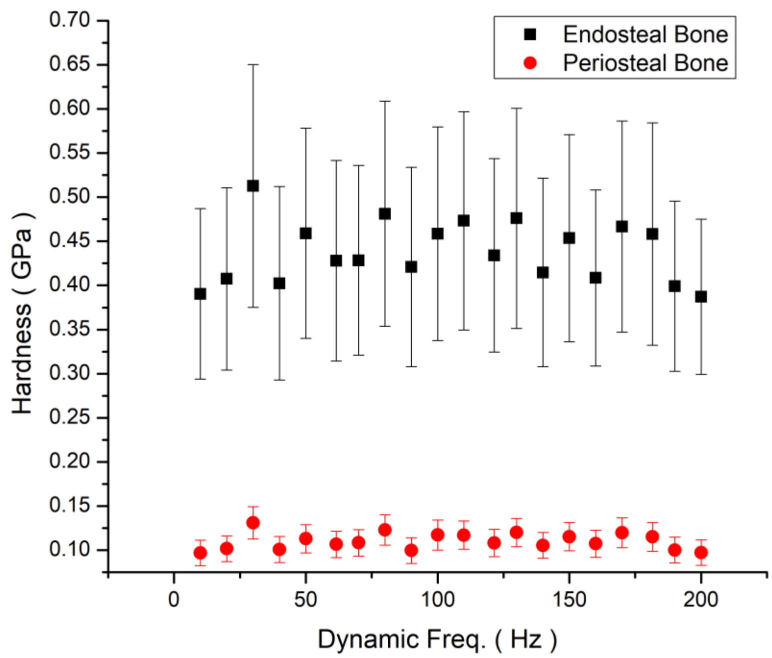

Figure A.12: Hardness - posterior quadrant of 4-week-old bone

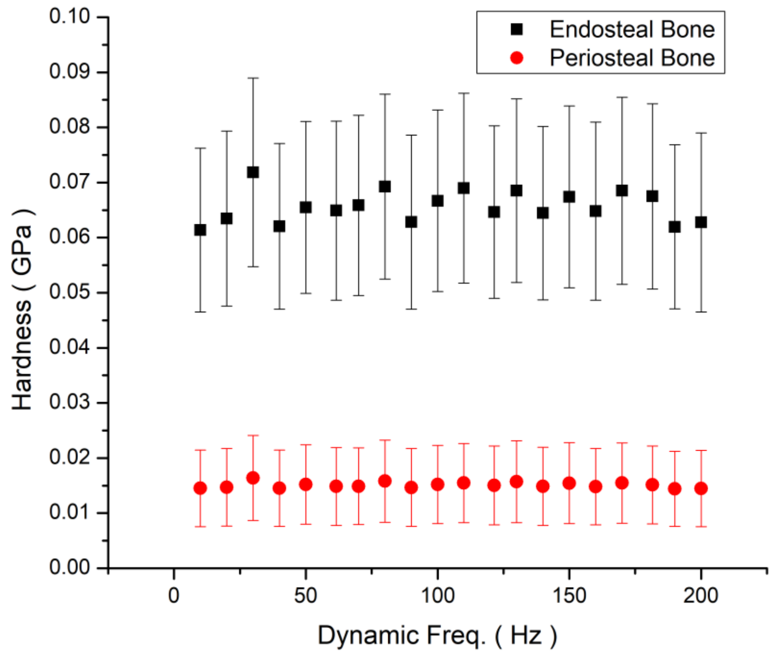

Figure A.13: Hardness - anterior quadrant of 16-week-old bone

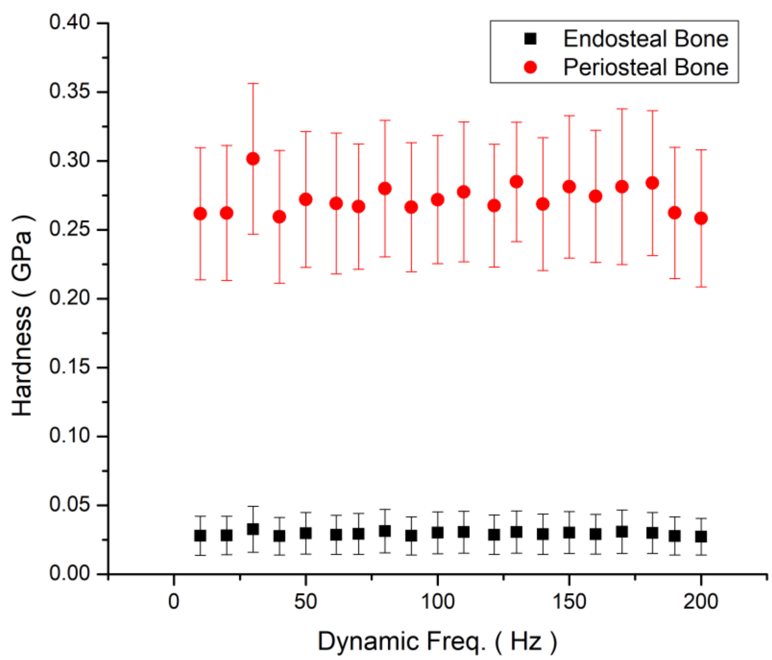

Figure A.14: Hardness - lateral quadrant of 16-week-old bone

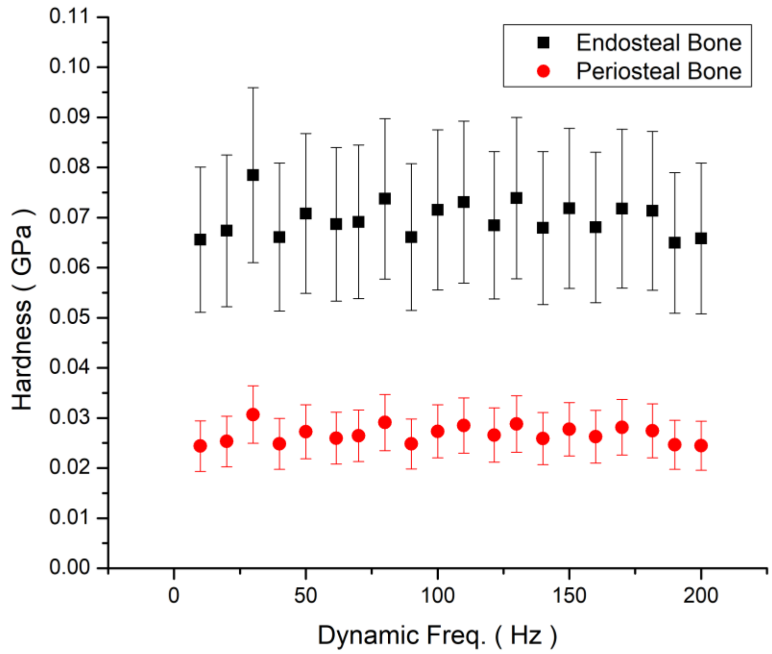

Figure A.15: Hardness - medial quadrant of 16-week-old bone

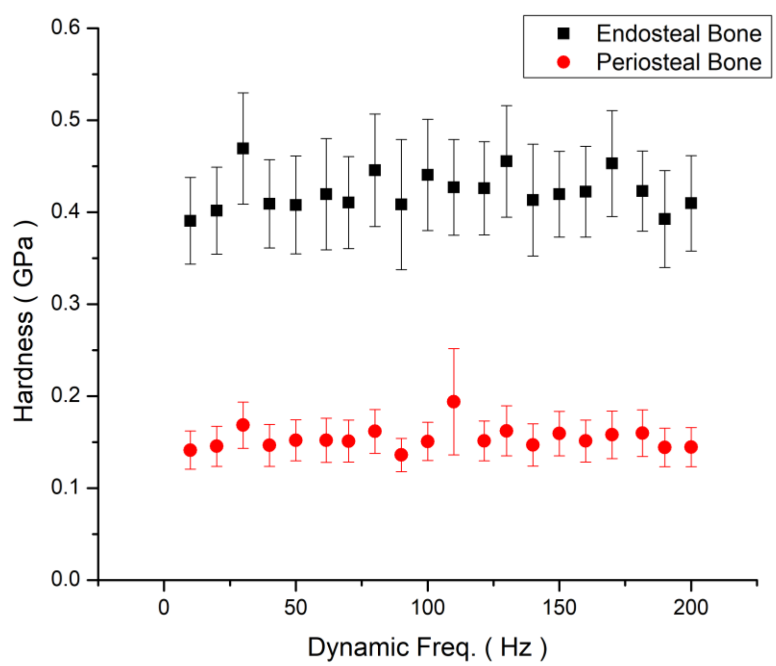

Figure A.16: Hardness - posterior quadrant of 16-week-old bone

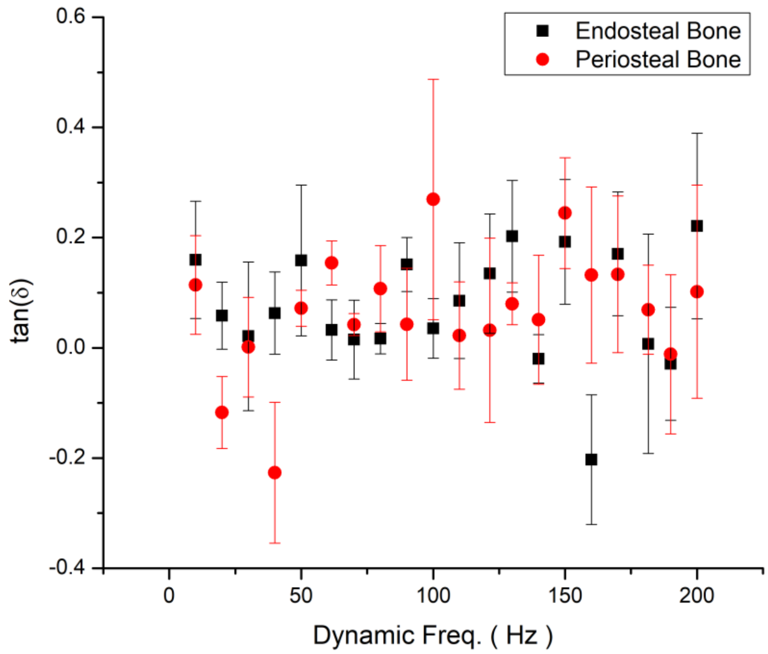

Figure A.17: tan-delta - anterior quadrant of 4-week-old bone

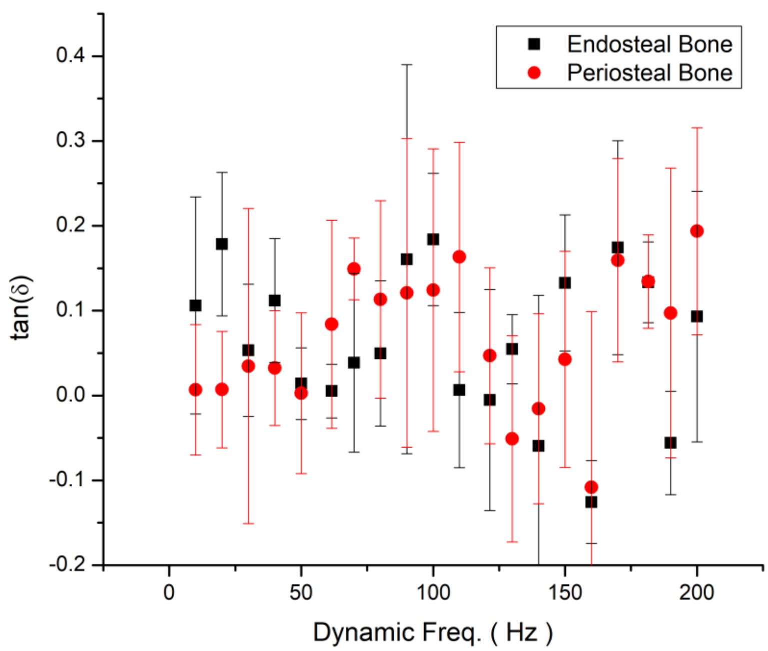

Figure A.18: tan-delta - lateral quadrant of 4-week-old bone

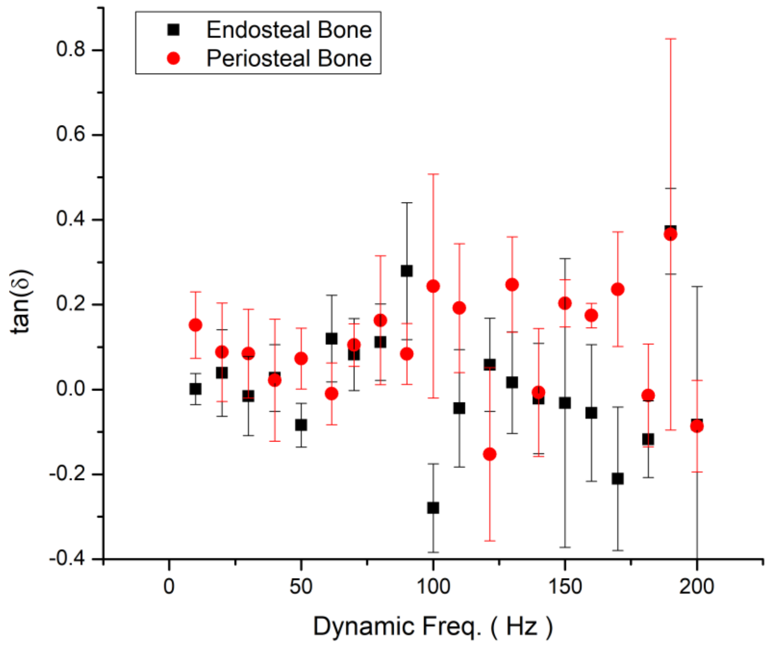

Figure A.19: tan-delta – medial quadrant of 4-week-old bone

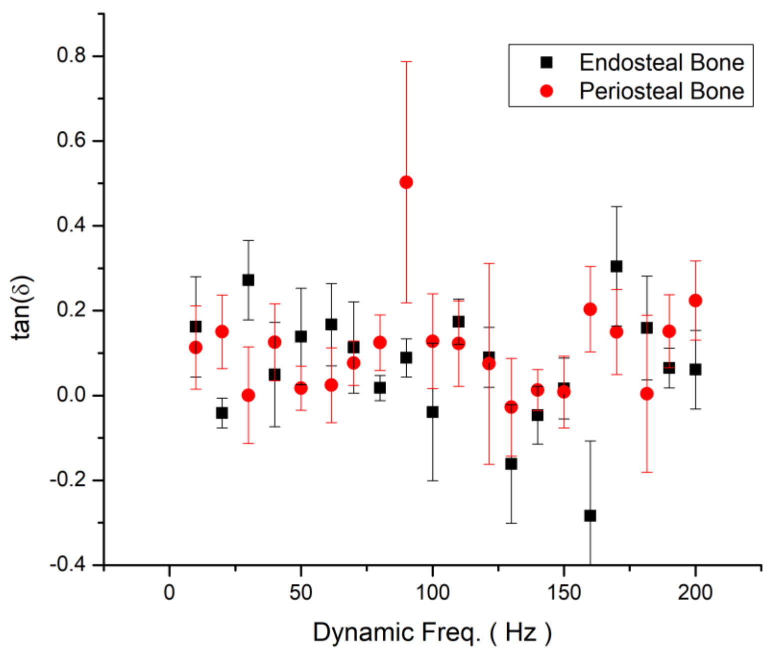

Figure A.20: tan-delta - posterior quadrant of 4-week-old bone

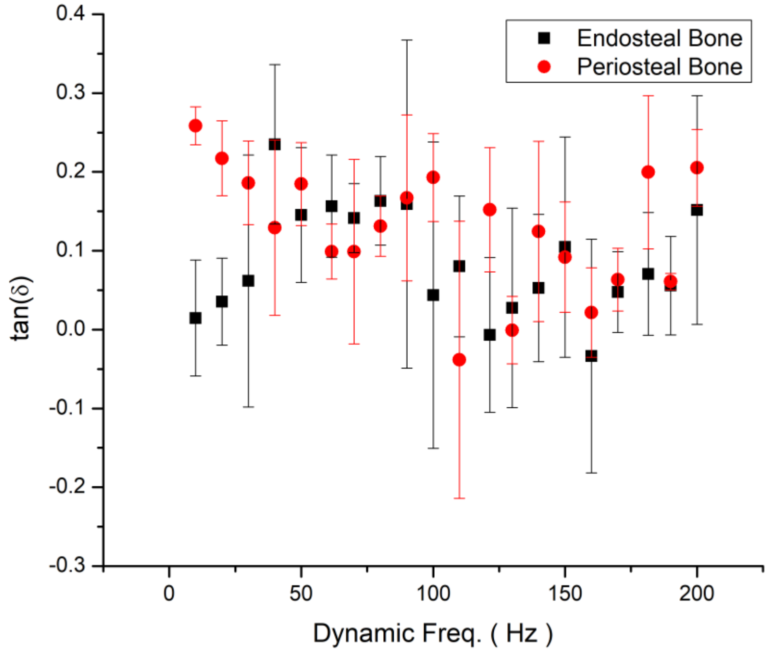

Figure A.21: tan-delta - anterior quadrant of 16-week-old bone

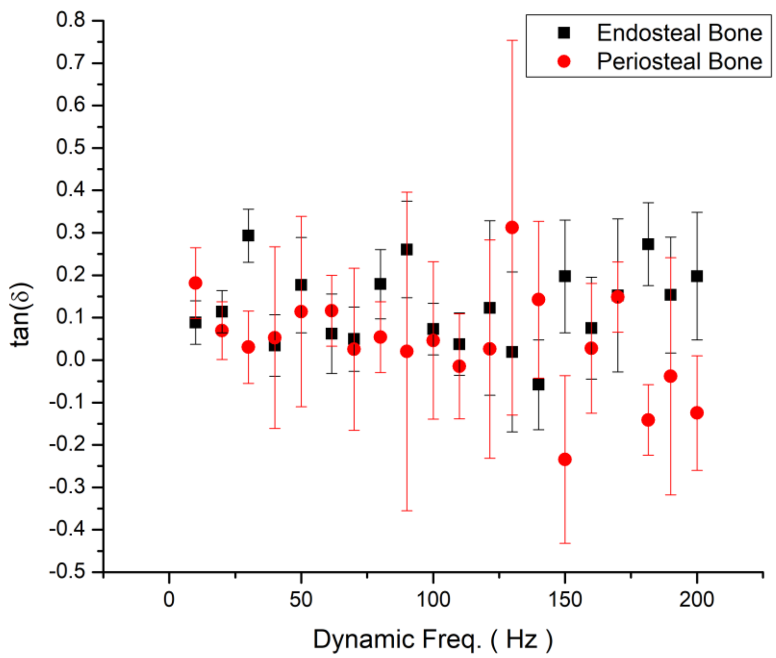

Figure A.22: tan-delta – medial quadrant of 16-week-old bone

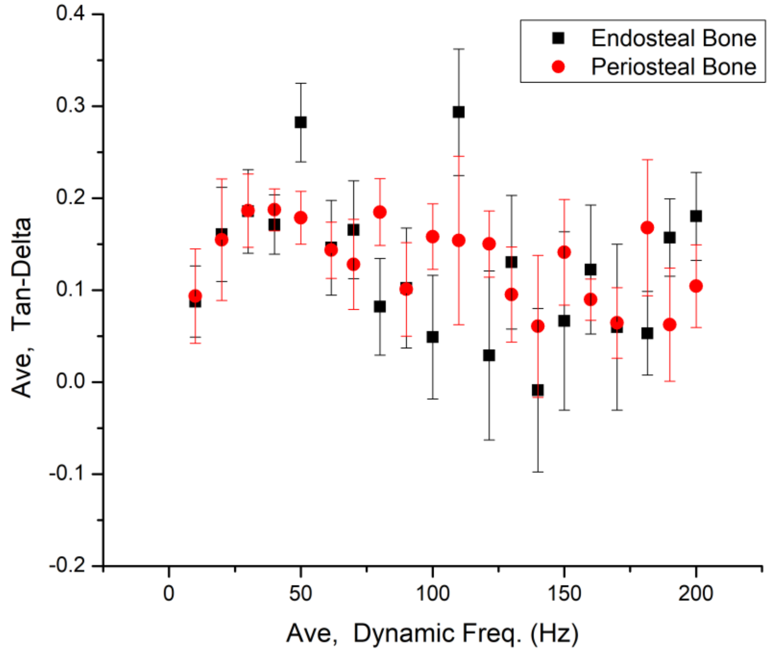

Figure A.23: tan-delta - lateral quadrant of 16-week-old bone

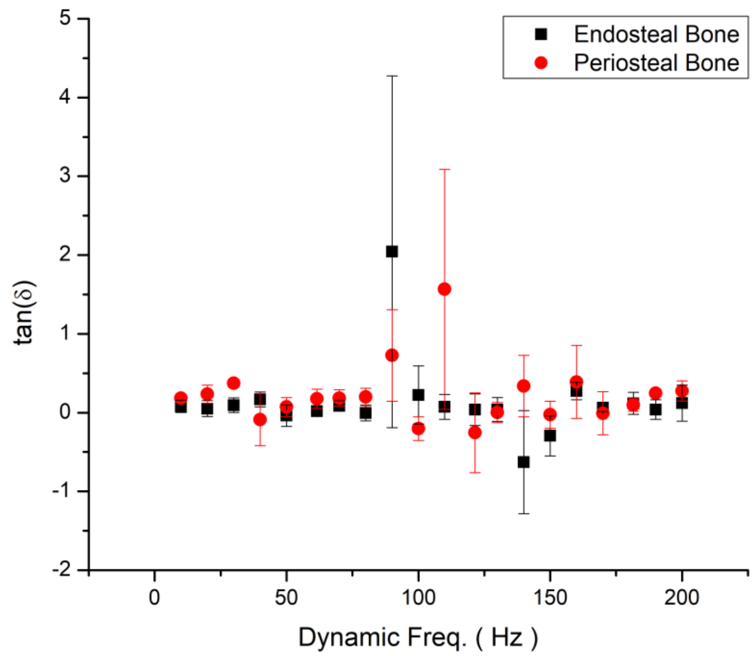

Figure A.24: tan-delta - posterior quadrant of 16-week-old bone